Peer reviewed version of the manuscript published in final form in Advanced Functional Materials (2020)

Assembly of Living Building Blocks to Engineer Complex Tissues

*Liliang Ouyang, James P. K. Armstrong, Manuel Salmeron-Sanchez and Molly M. Stevens**

Dr. L. Ouyang, Dr. J. P. K. Armstrong, Prof. M. M. Stevens
Department of Materials
Department of Bioengineering
Institute of Biomedical Engineering
Imperial College London
London, SW7 2AZ, UK

Prof. M. Salmeron-Sanchez
Centre for the Cellular Microenvironment
University of Glasgow
Glasgow, G12 8LT, UK

*E-mail: m.stevens@imperial.ac.uk

Abstract

The great demand for tissue and organ grafts, compounded by an ageing demographic and a shortage of available donors, has driven the development of bioengineering approaches that can generate biomimetic tissues *in vitro*. Despite the considerable progress in conventional scaffold-based tissue engineering, the recreation of physiological complexity has remained a challenge. Bottom-up tissue engineering strategies have opened up a new avenue for the modular assembly of living building blocks into customized tissue architectures. This Progress Report will overview the recent progress and trends in the fabrication and assembly of living building blocks, with a key highlight on emerging bioprinting technologies that can be used for modular assembly and complexity in tissue engineering. By summarizing the work to date, providing new classifications of different living building blocks, highlighting state-of-the-art research and trends, and offering personal perspectives on future opportunities, this Progress Report aims to aid and inspire other researchers working in the field of modular tissue engineering.

Keywords: living building blocks; biofabrication; assembly; bottom-up tissue engineering; bioprinting

1. The Emergence of Modular Tissue Engineering Strategies

The past three decades have seen the development of different methods for engineering *in vitro* constructs that can be used to restore, maintain, or model the function of natural tissues and organs. [1-3] Typically, hydrogels or solid scaffolds are seeded with cells and presented with growth factors that can regulate cell differentiation and/or extracellular matrix production. [4] This top-down strategy offers a high-throughput method for engineering relatively small and simple tissue constructs, however, issues can arise when applying these approaches to larger and more complex structures. [5, 6] For example, it can often be challenging to seed cells on macroscale scaffolds with a uniform distribution and at densities that match native tissues. Further challenges arise when seeking to generate spatially-organized multicellular structures or complex tissue features (*e.g.*, aligned cells/fibers, vasculature, neural junctions, musculoskeletal interfaces, zonal/gradient transitions). [7] These considerations have led, in part, to the development of bottom-up tissue engineering strategies based on the modular assembly of non-living and living building blocks (**Figure 1A**). [8, 9] This approach is inherently scalable and provides a more versatile route to engineering tissue structures of higher architectural, compositional and cellular complexity. In general, this strategy opens up new avenues for engineering complex tissues with control over both the microscale units and the macroscale structure.

Past reviews have described a general overview of modular assembly for bottom-up tissue engineering, [8-11] while others have provided a more focused view of specific building blocks [12, 13] or assembly techniques. [14-16] However, there have been a number of recent advances in biofabrication that have significantly enriched the palette of available modules and assembly techniques. [17, 18] In this Progress Report, we provide a thorough account of the recent progress and trends in this area, with a focus on living building blocks, *i.e.* those comprising or containing viable cell populations. We first present a comprehensive summary of the different available living building blocks and how they can be fabricated

or engineered for tissue assembly. These examples span from single cell units to complex cellular modules, and are categorized here based on the building block dimensionality and the presence of a supporting material component. We consider the different methods that can be used for the self-assembly, directed assembly and remote assembly of living building blocks. In particular, we highlight recent prominent methods, such as molecular recognition, acoustic cell patterning and 3D bioprinting. Finally, we provide a set of critical perspectives regarding the unique trends, opportunities and challenges of bottom-up tissue engineering.

2. Fabricating Living Building Blocks

All modular tissue engineering strategies require the use of living building blocks, such as cell spheroids, cell sheets, or cell-laden microgels. [8] In this Progress Report, we present a new classification of living building blocks based on their dimensionality and the presence or absence of a supporting biomaterial (**Figure 1B**). Under this classification, we consider single cells as the base, zero-dimensional (0D) unit of any tissue engineering system. Single cells can either be assembled to form tissue structures or used to create higher-dimension living building blocks. These modules include cellularized structures with at least one high-aspect ratio (≥20) dimension, namely, one-dimensional (1D) fibers and two-dimensional (2D) sheets. Multicellular systems with low aspect ratio (<20) are considered here as three-dimensional (3D) modules, while cellularized building blocks that undergo temporal changes in geometry or cellular organization are defined as four-dimensional (4D) systems. We further classify these living building blocks based on whether they comprise just cells (*e.g.*, cell sheets, organoids) or contain a supporting biomaterial (*e.g.*, cellularized fibers, cellularized microgels). In this section, we will examine different methods that are used to fabricate living building blocks in each of these different categories (**Table 1**).

2.1. Single Cells

The base unit of all tissues are cells, which produce and remodel the extracellular matrix, secrete signalling factors and execute key functional roles (*e.g.*, sensing, contraction, insulin production). Cells can be used for tissue engineering immediately after harvest, alternatively, various modification strategies can be employed to augment the function of cells as living building blocks. For example, cells can be differentiated, transdifferentiated, or reprogrammed to an induced pluripotent state, using biochemical factors, material cues, or transgene expression of key transcription factors. Meanwhile, the development of CRISPR/Cas and related technologies has enabled high precision genome editing.[19] An alternative to biological engineering is cell membrane functionalization (**Figure 2A**).[20, 21] For instance, covalent modifications can be made using enzymes or certain cytocompatible chemical reactions.[22-24] This is achieved by modifying natural functional groups present on the cytoplasmic membrane, alternatively, bio-orthogonal reactions can be performed on unnatural reactive handles (*e.g.*, azides), introduced using metabolic labelling.[25] Non-covalent bonds can also be used to guide cell functionalization, for example, cationic nanomaterials can electrostatically bind to anionic proteoglycans on the cell surface,[26, 27] while hydrophobic groups can anchor into the phospholipid membrane bilayer.[28-31]

2.2. Cell Fibers

1D cell fibers are usually generated using micropatterned substrates. For example, Gantumur *et al.* used an inkjet printing process to fabricate culture surfaces with adhesive and non-adhesive regions for selective cell attachment (**Figure 2B**).[32] These substrates were used to form patterned lines of fibroblast-like cells, which could subsequently be released as free-floating cell fibers by degrading the underlying substrate. Microtopography has also been used to fabricate cell fibers. For example, Mubyana and Corr showed that microchannels could be used to generate lines of fibroblasts, which could be released into suspension as single tendon fibers through the application of tensile loads.[33] Cell fibers

can also be templated using core-shell structures that are generated using coaxial laminar flow of hydrogel precursors and a corresponding crosslinker (*e.g.*, sodium alginate and calcium chloride). For example, Ozbolat and colleagues post-seeded fibroblasts into the core of a calcium-alginate hydrogel capsule. This system was cultured for 5-7 days to form dense cell fibers that could be released by degrading the alginate shell using sodium citrate. [34, 35] These contrasting approaches each have their own advantages; while surface patterning is relatively simple and high throughput, post-seeding into the lumen of a hydrogel capsule enables the generation of thicker fibers with a spherical cross-section.

2.3. Cell Sheets

The production of 2D cell sheets date back to the 1990s, when Okano and colleagues were investigating the use of culture surfaces grafted with poly(*N*-isopropylacrylamide). [36, 37] These coatings are hydrophobic at 37 °C but become hydrophilic below the lower critical solution temperature of the polymer (25 °C in PBS). These switchable surfaces were used to generate confluent layers of cells (*e.g.* endothelial cells, hepatocytes, pluripotent stem cells) at 37 °C, which could then be detached into floating cell sheets simply by decreasing the temperature (**Figure 2C**). [38, 39] Various other detachment mechanisms have been investigated, including methods based on enzymatic cleavage, electrochemical polarization, and pH changes. [39-41] Concurrently, other groups have focused on the generation of structurally complex cell sheets. Rim *et al*. used hydrogels with microgrooves to orient vascular smooth muscle cells, which were released as aligned cell sheets by degrading the underlying substrate. [42] Liu *et al.* used culture substrates containing TiO_2 nanodots, which could be used to increase the surface wettability by irradiating the substrate with ultraviolet light. This process was used to detach isotropic sheets of pre-osteoblastic cells, moreover, pre-irradiating the nanodots with a patterned photomask could be used to spatially modulate protein adsorption and obtain sheets of aligned human foreskin fibroblasts. [43]

2.4. Cell Spheroids

Certain culture conditions can be used to encourage cells to aggregate into 3D spheroids. Suspension culture, which uses non-adherent substrates or cells, can be used as a high-throughput method for producing 3D cell aggregates. [44] The stochastic nature of this aggregation process can result in high polydispersity, however, uniformity can be improved by using spinning or rotation culture methods. [45-47] A higher degree of control over individual spheroids can be attained by using hanging-drop culture, although this approach is considered to be technically challenging and low throughput. [48] On the other hand, culturing cells using micropatterned or microwell substrates offers a simple, high-throughput method with relatively high control over the spheroid size. [15] An alternative to cell aggregation was proposed by Sun and colleagues, who showed that the proliferation of single cells embedded in a patterned hydrogel could be used to generate cell spheroids with high uniformity and yield (**Figure 2D**). [49-51] Moreover, the cell spheroids could be released upon reaching the desired size simply by degrading the surrounding hydrogel. Single-cell proliferation is also likely to produce spheroids with a more homogeneous phenotype compared to those formed by aggregating potentially heterogenous cell populations. Another alternative to cell aggregation was reported by Wang *et al.*, who showed that hollow cell spheroids could be formed by creating epithelial cell monolayers on the surface walls of a spherical hydrogel chamber. [52]

2.5. Cell Organoids

Many of the techniques used in spheroid culture can be applied to the generation of cell organoids; complex cell structures that mimic the structural and functional aspects of organs, such as the intestine, brain, stomach, lung, liver, and kidney. [53] Organoids exhibit dynamic stem cell self-renewal and tissue organization, it is these temporal changes in structure and biology that defines their classification as 4D living building blocks. The organization of cells into layers and tissue regions can occur spontaneously

or it can be guided by biochemical or biophysical cues. [7, 54] For example, Lancaster *et al.* used poly(lactic-*co*-glycolic acid) (PLGA) microfilaments as floating scaffolds to culture elongated embryoid bodies (EBs) that form cerebral organoids with enhanced cortical development. [55] Meanwhile, Gjorevski *et al.* introduced biochemically and mechanically tunable PEG hydrogels for the culture of intestinal organoids. The authors observed that high-stiffness matrices coupled with fibronectin-based adhesion significantly enhanced intestinal stem cells expansion, while the formation of intestinal organoids required a soft matrix and laminin-based adhesion (**Figure 2E**). [56] Recently, different approaches have been used to enhance the vasculogenesis of organoids, using flow shear stress [57] or cell co-culture. [58] Although biomaterials are often used to assist cell organization and development, the resulting organoids can be generally harvested as scaffold-free cellularized structures. Organoids offer an exciting opportunity for the modular assembly of complex tissues, as they provide a living building block with a more advanced structure and biological relevance than individual cells or simple cell aggregates. [53]

2.6. Single-Cell-Laden Microgels

Thus far, we have considered biomaterial-free living building blocks, however, each of these systems also has a cellularized biomaterial counterpart. Even the base unit of individual cells can be formulated as single-cell-laden microgels, a strategy that has recently emerged for tissue engineering, regenerative medicine, and the study of cell-niche interactions. [59] Most of the current methods employ microfluidic assemblies that generate water-in-oil emulsion microdroplets, however, it can be technically challenging to produce microgels containing just one cell. Indeed, the number of encapsulated cells per microgel inherently follows the Poisson distribution, resulting in maximum 37% single-cell-laden microgels. [59-62] Fluorescence-activated cell sorting can be used to filter out cell-free microgels, an approach that has been used to generate single-cell-laden microgel populations with over 70% purity. [63] More recently, Mooney and colleagues reported a selective crosslinking strategy in which cells were membrane-

functionalized with $CaCO_3$ nanoparticles, with the released calcium ions capable of crosslinking alginate [64] or acting as a cofactor for the enzymatic crosslinking of PEG hydrogels (**Figure 2F**). [65] This strategy produced a single-cell-laden microgel purity of up to 91 ± 7% [65] with extremely thin hydrogel layers surrounding each cell (average 5.8 μm). [64] Meanwhile, it was demonstrated that delayed enzymatic crosslinking [62] and orbital shaking of cell-laden emulsion droplets [65] could effectively prevent cell egress and position single cells at the centre of fabricated microgels.

2.7. Cellularized Biomaterial Fibers

Molding offers a relatively simple approach for fabricating 1D cellularized biomaterial fibers. For example, Neal *et al.* used a gelatin-based mold to cast fibrin hydrogel fibers laden with a high density of myoblasts, which could be aligned using uniaxial tensile loads. [66] Microfluidics offers a more complex but higher throughput alternative. Due to its rapid gelation kinetics in the presence of divalent cations (*e.g.*, Ca^{2+}), alginate is commonly used, either alone or doped with other biopolymers. For example, capillary-based and chip-based multi-channel microfluidic devices have been used to fabricate cellularized alginate fibers with multicomponent, core-shell, and spindle-knot structures (**Figure 2G**). [67-70] Notably, Kang *et al.* developed a microfluidic system with a digital flow control for generating coded cellularized alginate fibers with tunable morphological, structural and chemical features, [68] while Onoe *et al.* used microfluidics with double-coaxial laminar flow to fabricate meter-long core-shell cellularized alginate fibers encapsulating a core of ECM hydrogel. [71] Other biopolymers and crosslinking mechanisms can also be used to generate cellularized fibers. For example, Daniele *et al.* used a UV curing window at the end of a core-shell microfluidic device to photocrosslink cellularized poly(ethylene glycol) dimethacrylate (PEGDMA) into continuous fibers. [72] In another study, cell-laden phenolic-substituted hyaluronic acid (HA-Ph) was crosslinked into cellularized fibers with an ambient flow of H_2O_2 and a horseradish peroxidase (HRP)-catalyzed reaction. [73] An alternative approach is to use wet-spinning or extrusion, relatively simple methods that can be applied to many different

biomaterials, such as GelMA, PEGDA, MeHA, and κ-carrageenan. [74-77] For example, Zhang *et al.* produced aligned cell-laden monodomain gel fibers by exploiting the self-assembly of peptide amphiphiles during extrusion into a salt solution. [78] More recently, cell electrospinning has been introduced for generating thin cellularized biomaterial fibers. Despite the use of high voltages, cell viabilities exceeding 80% have been reported for electrospun alginate, collagen, and Matrigel. [79, 80]

2.8. Cellularized Biomaterial Sheets

A simple strategy for creating 2D cellularized biomaterial sheets is to culture cells on top of an adherent sheet substrate. For example, Nam *et al.* fabricated aligned collagen sheets by continuous cyclic stretching, which supported the alignment of cultured corneal stromal cells and smooth muscle cells. [81] An alternative strategy was proposed by Yajima *et al.*, who generated 100-150 μm thick cellularized sheets by the aggregation of cells and cell-sized collagen microparticles on a non-adherent surface after 1 day in culture (**Figure 2H**). [82] A more conventional approach is micromolding, which can be used to generate patterned hydrogel sheets. For example, Bursac and colleagues used polydimethylsiloxane (PDMS) molds with arrays of mesoscopic posts to guide local cell alignment in fibrin and Matrigel hydrogels and produce 100-400 μm thick sheets of muscle [83] and cardiac tissue. [84] Similarly, Son *et al.* used customized PDMS molds to fabricate micropatterned cell-laden alginate hydrogel sheets with a thickness of approximately 100-140 μm. [85] More dynamic control over sheet fabrication can be achieved using microfluidics. For example, Leng *et al.* used a microfluidic device with programmed valve actuation to controllably incorporate payloads (*e.g.*, living cells) into a layer of base biomaterial (*e.g.*, alginate) to produce mosaic hydrogel sheets with a thickness of 150-350 μm. [86] In another study, Kobayashi *et al.* used a multichannel microfluidic device to prepare alginate sheets, of thickness 90-100 μm, containing a high density of hepatocytes and fibroblasts in an alternating stripe pattern. [87]

2.9. Cellularized Microcarriers

Many of the approaches used to generate high-aspect-ratio structures can also be applied to the fabrication of low-aspect-ratio 3D cellularized biomaterials. The primary targets are cell-seeded porous microparticles/microscaffolds [88, 89] and cellularized microgels. [90] Microgels have been fabricated using a variety of biomaterials with different gelation mechanisms, including alginate, [91, 92] agarose, [93] methacrylated hyaluronic acid, [94] poly(ethylene glycol) diacrylate (PEGDA), [95] poly(ethylene glycol) maleimide (PEGMAL), [96] GelMA, [97] self-assembled peptides, [98, 99] and tissue-specific extracellular matrix (ECM). [100] Two-phase emulsions (*e.g.*, water-in-oil) can be used to template the formation of microgels. [52] While this method is simple and high throughput, it generally produces microgels with a polydisperse size distribution. Greater uniformity can be achieved using laminar flow-focusing methods (**Figure 2I**). [90, 97] A common system is the use of calcium ions to form crosslinked alginate microgels, however, other cellularized biomaterials can also be used by applying the gelation triggers in a contact [96] or non-contact fashion. [93] For example, agarose microdroplets can be set by cooling, [93] ECM and collagen microgels can be gelled by heating (generally to 37 °C), [100] while GelMA microdroplets can be photocrosslinked by UV irradiation. [101] Other fabrication methods include electro-assisted jetting and inkjet printing, [102-104] while micromolding [105] and photolithography [106-109] have been used to produce non-spherical microgels. For example, customized photomasks and photo-crosslinkable hydrogel precursors have been used to generate microgels with triangle, star, hexagon, and gear-like geometries. [108]

2.10. Shape-Changing Cellularized Biomaterials

The ability of cell-laden 3D modules to undergo temporal changes in shape defines their classification as a 4D cellularized biomaterial. Controlled shape changes can be mediated by using layered materials, in which the difference in swelling or shrinking between two layers results in programmed shifts in

geometry. [110-112] For example, Jamal *et al.* used photolithography method to fabricate cell-laden bilayers containing PEGDA of different molecular weights. These structures predictably folded into spherical capsules, helices, and cylindrical hydrogels upon swelling in aqueous media. [111] By using poly(*N*-isopropylacrylamide), a thermosensitive polymer that can undergo phase transitions at relatively mild temperatures, Stroganov *et al.* produced bilayer structures that could undergo reversible shape changes. [112] Notably, this system could be used to trap and release cells by using temperature changes to instigate folding (>28℃) and unfolding (20℃). Shape-changing hydrogels have also been demonstrated using single-component systems. For example, Kirillova *et al.* printed, crosslinked and then dried thin layers of methacrylated hyaluronic acid or alginate, which folded into tubular structures after immersion in aqueous media. [113] The authors suggested that the folding mechanism was driven by depth-dependent differences in crosslinking density. An alternative mechanism for driving biomaterial shape changes is to harness the traction force generated by adherent cells. For example, Kuribayashi-Shigetomi *et al.* showed that fibroblasts seeded on micropatterned parylene microplates would cause the underlying substrate to lift and fold into a prescribed geometry (**Figure 2J**). [114]

3. Self-assembly of Living Building Blocks

Self-assembly of living building blocks can occur through many different mechanisms, including chemical binding, physical interactions, biological adhesion, and geometric recognition. The key principle underpinning these self-assembly processes is that they are thermodynamically driven; *i.e.* the final assemblies have a lower Gibbs free energy than the dissociated building blocks. Generally, these strategies are also designed to have a low kinetic barrier, which enables the building blocks to be assembled under relatively mild conditions. Here, we summarize four of the major approaches for self-assembly of living building blocks (**Figure 1C**, **Table 2**).

3.1. Minimization of Surface Tension

Self-assembly can arise from the tendency of objects to minimize their surface area and the resulting surface free energy between different phases. The assembly of living objects based on this capillary force was pioneered by Khademhosseini and colleagues, who reported the self-assembly of fibroblast-laden poly(ethylene glycol) methacrylate (PEGMA) microgels in mineral oil (**Figure 3A**). [106] Random, branched and linear assemblies were obtained by varying parameters, such as microgel size, agitation rate, agitation time, and the presence of surfactant. A secondary photo-crosslinking step was used to stabilize the assemblies in absence of the oil phase. [106] Follow-up studies showed that this self-assembly process, driven by surface tension minimization of the living building blocks, could be guided by other interfaces. [115, 116] For example, cellularized PEG-based microgels are able to float to the top of a high-density hydrophobic solution (*e.g.*, CCl_4), self-assemble at the liquid-air interface and undergo photocrosslinking to yield cellularized hydrogel sheets. [116] Moreover, porous hydrogel constructs can be made by co-assembling cell-laden PEG-based microgels with alginate microgels, with the latter acting as a sacrificial template for pore production. [117] In a more recent study, Wei *et al.* reported that the inclusion of methacrylated alginate (AlgMA) could be used to increase the hydrophilicity of cellularized GelMA microgels and promote enhanced self-assembly in mineral oil. [118] In general, surface tension can be used as a simple and rapid means of self-assembling centimeter-scale building blocks[117] but is limited for more customized assembly applications.

3.2. Geometric Recognition

More control can be leveraged by using geometric recognition; in which living building blocks of particular shapes preferentially self-assemble. [119] For example, in a mineral oil bulk phase, cross-shaped microgels can trap rod-shaped microgels in a ‘lock-and-key’ conformation, [106, 116] while ring-shaped microgels can self-assemble into concentric double-ring structures. [118] As a proof-of-concept, this process was used to create integrated assemblies of microgels loaded with either osteosarcoma cells or

endothelial cells. [118] A slightly different approach was taken by Eng *et al.*, in an impressive recent report on shape-defined self-assembly (**Figure 3B**). [120] The authors fabricated circular, triangular and rectangular cell-laden GelMA microgels (100-1000 μm in size), which were then subjected to repeated sedimentation-resuspension steps with a patterned gel containing shape-matched well features. Up to 90% of the microgels were correctly docked when using microgels that were 85% the size of the congruent wells. The precision self-assembly of coded microgels, embedded with different cell types, was used to study the diffusive cell-cell communication during vasculogenic network formation in shape-defined co-cultures of human mesenchymal stem cells (MSCs) and human endothelial cells (ECs). [120] Geometric recognition has also been used to guide the remote assembly of living building blocks in acoustic [121] and magnetic fields [122] (see **Section 5.1** and **5.2**). Overall, geometric recognition enables a more pre-programmed self-assembly route, however, the need to fabricate customized shape-defined building blocks is a limitation of this approach.

3.3. Molecular Recognition

We have thus far only considered mechanisms that use physical interactions to guide self-assembly. The advantage of these strategies is that unfunctionalized living building blocks can be used, on the other hand, the use of non-specific interactions restricts highly programmed self-assembly. This can be addressed by using molecular recognition, in which living building blocks are assembled using specific chemical interactions. The most common approach is to use biorthogonal reactive groups, such as oxyamines and ketones, [123, 124] azides and alkynes, [125] or thiols and alkenes. [126, 127] For example, Liu *et al.* reported the self-assembly of cell-laden PEGDA microgels into porous hydrogel constructs in the presence of thiolated polypeptide crosslinkers. [126] The authors observed that the star-shaped modules produced constructs with a higher porosity, permeability, and pore interconnectivity than assemblies of circle- and square-shaped microgels. Meanwhile, Li *et al.* functionalized cell-laden PEGDA microgels with single-stranded DNA (ssDNA), which self-assembled *via* sequence-specific hybridization. [128]

These principles have been extended to cellular self-assembly by using membrane-functionalized cells. For example, Gartner and colleagues grafted complementary ssDNA strands onto the surface of different metabolically-labelled cell populations. This enabled the programmed synthesis of multilayer clusters or layer-by-layer structures sequentially assembled and grown outward from a surface (**Figure 3C**). [20, 129]

3.4. Biological Interactions

While molecular recognition relies on careful surface functionalization strategies, cells naturally exhibit biological adhesion mechanisms that can enable cell-cell interactions and cellular fusion. Cell-cell interactions are predominantly mediated by the binding of cell adhesion molecules, such as cadherins, a ubiquitous feature of the cytoplasmic membrane. [130] However, there are other factors that can regulate the self-assembly of cells. For example, Morgan and colleagues observed reduced aggregation in cells treated with an inhibitor of Rho kinase, which suggested that cytoskeletal-mediated contraction is important for cell-cell adhesion. [131] Morgan and colleagues further investigated factors governing the fusion of cell spheroids. [132] Notably, they observed that a longer pre-culture time for the spheroids resulted in slower fusion and reduced coherence, which was attributed to the spheroids increasing in viscoelasticity during culture. Other groups have focused on the assembly of more complex cell modules. For example, Kato-Negishi *et al.* observed cell-cell adhesion and synaptic connectivity between adjacent rod-shaped neural units. [133] These principles have been further extended to the fusion of organoids, in order to assemble large and complex microtissues. For example, the fusion of intestinal organoids has been used to generate centimeter-scale interconnected epithelial tubes. [134] Meanwhile, several groups have used spontaneous fusion of cerebral organoids to generate hybrid brain microtissues exhibiting complex biological structure and function (**Figure 3D**). [135-137] For instance, Bagley *et al.* showed that cerebral organoids of dorsal and ventral forebrain identity could be assembled to create a dorsal-ventral axis for directional interneuron migration. [136]

4. Directed Assembly of Living Building Blocks

Self-assembly benefits from spontaneous interaction, however, a greater degree of customization can be achieved when using some form of energetic input during the assembly process. These directed assembly methods can be highly manual, such as packing, bundling, and stacking, or more automated, such as the use of weaving, knitting or braiding to produce interlaced material assemblies. Most notably, bioprinting has emerged as a versatile, automated technique for constructing custom 3D assemblies of living building blocks. Here, we outline five of the major approaches for the directed assembly of living building blocks (**Figure 1C**, **Table 2**).

4.1. Packing

The simplest approach to directed assembly is to pack living building blocks within a confined space. Although this method can be applied to any living building block, it has the most relevance for cell spheroids [132] and cellularized microcarriers. [88, 89, 138, 139] Cells can be packed into shaped molds, however, the released structure will often compact and adopt a spherical geometry over time due to the lowest energy principle. [140] This issue was discussed by Vrij *et al.*, who also showed that spheroids packed into shaped microwells could be used to generate larger structures that retained their templated geometry. [141] This approach can be used either to form non-spherical living building blocks or to engineer material-free tissue constructs (*e.g.*, middle-ear bone). [141] A similar method had previously been presented by Rago *et al.*, who showed that trough-shaped molds could be used to generate cylindrical tissue constructs from fused human fibroblast spheroids. [132] Lin *et al.* packed 6.5 mm Transwell inserts with neural spheroids derived from human induced pluripotent stem cells (iPSC), which fused and differentiated to form midbrain dopaminergic or cortical neural tissue. [142] This report also showed that spheroids in the later stages of neural differentiation exhibited a reduced rate of fusion, compared to those in the early stages of culture.

Cell-laden microcarriers can also be used to provide structural support to cells or to generate interstitial pores for perfusion culture. This approach was taken by McGuigan *et al.*, who showed that rod-shaped collagen microgels could be packed in a large tube (~5 mm in diameter) to create a porous structure that could be cultured under continuous flow. The authors used this method for vascular tissue engineering by creating packed assemblies of microgels containing liver cell lines, coated with a confluent layer of endothelial cells. [138, 139] A similar method was used by Khan *et al.*, who packed cellularized collagen modules in an organ-shaped chamber. [143] This approach can also be applied by using porous microparticles seeded with cells as the living building block. [88] For example, Wang *et al*. generated packed, centimeter-scale constructs using microparticles seeded with MSCs, fibroblasts or liver cell lines, which were cultured for 14 days under perfusion. [88] Packing has also been used to construct tissue out of non-hydrogel living building blocks. For example, Leferink *et al.* showed that SU-8 microcubes [89] or poly(D,L-lactic acid) microscaffolds [144] could be seeded with cells and subsequently assembled in non-adherent agarose microwells of different shapes and sizes (**Figure 4A**). Meanwhile, Pang *et al.* fabricated hollow polycaprolactone (PCL) microscaffolds, which were coated with collagen, seeded with a liver cell line, and then packed into a perfusion chamber for liver tissue engineering. [145]

4.2. Bundling

Bundling can be considered as an ordered packing approach for 1D living building blocks, such as cell-laden hydrogel fibers. [73, 146, 147] For example, Leong *et al.* used interfacial polyelectrolyte complexation to fabricate cellularized chitin-alginate fibers, which were bundled into a secondary fiber assembly with endothelial cells in the center. [146] Subsequent spooling was used to produce a tertiary, prevascularized microtissue with aligned vessels formed after 24 h of *in vitro* culture, which underwent anastomosis with the host circulation in a subcutaneous mouse model. The authors also demonstrated the formation of prevascularized adipose and hepatic tissue by co-bundling fibers bearing the respective cell types (**Figure 4B**). [146] More recently, Khanmohammadi *et al.* reported the fabrication of viable cellular constructs

made from bundled cell-laden hyaluronic acid fibers. [73] In another study, a liver cell line was densely loaded in the core of core-shell alginate fibers, which were then externally seeded with endothelial cells and bundled together for perfusion culture. The authors showed the formation of conduits resembling vascular networks between adjacent fibers in the bundled tissue constructs. [147] Moreover, Patil *et al.* showed that aligned cell fibers, tethered on a PDMS frame, could bundle together when lifted out of the culture medium. This process, mediated by capillary forces, was used to engineer aligned bundles of skeletal muscle. [148] This example highlights how fiber bundling can be used to generate tissue constructs with anisotropic properties.

4.3. Stacking

Stacking is another example of an ordered packing process, most commonly used for the assembly of 2D living building blocks. [85, 149-151] This approach was pioneered by Zimmermann *et al.*, who reported that cell-seeded collagen rings could be stacked into large, multiloop force-generating cardiac tissue constructs. When tested *in vivo* in an immunosuppressed rat model, these grafts showed non-delayed electrical coupling to the native myocardium 28 days after implantation. [152] More recently, Whitesides and colleagues developed a "cell-in-gels-in-paper" system, in which fibrous paper was printed with a hydrophobic pattern to enable selective attachment of cells from a layer of Matrigel. These cellularized sheets were stacked on top of each other to create uniform arrays of multilayered tissues. [153-155] An interesting stacking method was reported by Son *et al.*, who used a PDMS drainage well to precisely align the mesh pores of cell-laden, micropatterned hydrogel sheets during the assembly of multilayered constructs. [85] Meanwhile, Fukuda and colleagues recently reported the stacking of cell-laden microgels (*e.g.*, alginate or PEGDA) with a centered hole onto a rod collector. [107] Using microgels embedded with a liver cell line and coated with fibroblasts, the authors engineered a tissue mimicking a 3D hepatic lobule. [109]

Stacking can also be applied for the assembly of material-free building blocks, such as monolayer cell sheets. [149, 150] Haraguchi *et al.* reported the fabrication of dense cardiac tissue constructs by stacking monolayer cell sheets either manually or using a customized manipulator (**Figure 4C**). [149] This approach was also used to generate heterogeneous tissue structures by stacking sheets of different cell types, such as endothelial cells and myoblasts. [149] Stacking can also be used in combination with rolling to create multilayer tubular tissue constructs. For example, Gauvin *et al.* created vascular media and adventitia by using a tubular support to sequentially roll cell sheets obtained from the monolayer culture of smooth muscle cells and fibroblasts, respectively. [156] A more automated approach was reported by Othman *et al.*, who used a customized device to co-ordinate the rolling of different sheets into tubular architectures in an accurate and reproducible manner. [157] Using this method they showed that cell sheets and cell-laden hydrogel sheets could be assembled into multiwalled vessel constructs with arterial-like cell patterning and gut-like barrier function. Very recently, Ouyang *et al*. used diffusion-induced gelation to grow and stack up to seven different layers of cell-laden hydrogels onto a customized sacrificial template for the engineering of heterogeneous, branched vasculature. [158] Overall, stacking offers an attractive, albeit technically limited, method for the modular assembly of zonally-organized or multilayered tissues.

4.4. Textile-based Assembly

Several techniques from the textile industry have been applied for the fabrication of polymeric and collagen-based scaffolds for tissue engineering. [159-162] Indeed, many of these approaches have already been discussed in detail in several excellent reviews. [17, 163] However, the assembly of living building blocks using textile-based techniques has been more challenging as these processes must be adapted to perform under biocompatible conditions. One impressive example of a weaving-based approach was reported by Onoe *et al.*, who produced meter-long, cellularized alginate-ECM hydrogel fibers that were woven in calcium-spiked medium. [71] Ten different cellularized fibers were reported, including those seeded with fibroblasts, myoblasts, cardiomyocytes, endothelial cells, nerve cells, and epithelial cells,

and were used in a co-weaving approach to generate composite tissue structures (**Figure 4D**). [71] Akbari *et al.* introduced a more generalized approach in which a polypropylene strand was coated with a layer of cell-laden alginate. [164] The authors assembled these fibers using an array of common textile-based techniques, such as weaving, knitting, braiding, winding and embroidering. This principle was recently used by Costa-Almeida *et al.*, who braided suturing threads, coated with cell-laden alginate and GelMA hydrogels, into 3D constructs for tendon and ligament tissue engineering. [165] Textile-based techniques offer the opportunity for enhanced and anisotropic mechanical properties, however, more work is needed to fully explore the use of cellularized fibers as living building blocks.

4.5. Bioprinting

The emergence of bioprinting technologies has enabled the free form assembly of living building blocks for bottom-up tissue engineering. The concept of bioprinting is now well agreed upon by the community as "the use of computer-aided transfer processes for the patterning and assembly of living and non-living materials with a defined 2D or 3D architecture to produce bioengineered structures for regenerative medicine, pharmacokinetic and basic cell biology studies". [18, 166, 167] However, the terminology "bioink" has been divergent in terms of whether non-living formulations should be included. [166, 167] Nevertheless, in the context of this Progress Report, we will focus only on the use of cellularized bioinks. Indeed, different bioprinting technologies and their derivatives can be classified according to the shape of the living building blocks that are commonly used (**Table 3**). Here, we will focus on bioprinting techniques that generate and assemble biomaterial-based droplets, fibers, and sheets, and then highlight the recent progress made in biomaterial-free bioprinting.

Inkjet bioprinting, driven by heat or vibration, is a natural candidate for modular tissue assembly. This method allows the controlled deposition of cell-laden droplets into 2D or 3D constructs, with up to 90% cell viability. [168-170] For example, Hedegaard and colleagues recently used inkjet printing to guide the co-assembly of peptide amphiphiles with biomolecules in order to build up networks of microgels, which

could support viable cell populations. [170] Other droplet-based approaches include valve-based (*e.g.*, mechanical or solenoid valves), [171] laser-assisted, [172] and acoustic [173] bioprinting. For example, Sun and colleagues developed an alternating viscous and inertial force jetting system, which allowed them to print cell-laden droplets into defined 2D patterns [174] and into cell-laden hydrogels for the fabrication of heterogeneous tumor models. [175] Witte and colleagues used a microfluidic-based bioprinting approach to assemble pearl lace microgels laden with MSCs, which were stimulated to undergo osteogenesis by co-encapsulated non-pathogenic bacteria. [176] Droplet-based bioprinting enables rapid assembly at high resolution, with the latter achieved by assembling droplets down to picoliter volumes. [173] However, there are significant challenges, including structural instability caused by the typically low viscosity bioinks and evaporation of the deposited droplets. These challenges were addressed by Bayley and colleagues, who showed that cells could be printed as aqueous droplets into lipid-containing oil. The assembly was stabilized by the formation of droplet bilayer interfaces, enabling different model cell lines to be printed into a variety of complex 3D tissue architectures. [177]

Extrusion-based bioprinting has become the most widely used additive manufacturing approach in academia and industry because of its ease of use and ability to fabricate complex 3D tissue constructs. Driven by mechanical forces, pneumatic pressure or contact screw, liquid bioinks are extruded through a nozzle to generate fibers that are assembled layer-by-layer into customized 3D structures. [178] Bioink formulations must be extrudable, viscous enough to maintain fiber shape post-extrusion, and stable enough to support the assembly of multiple layers (**Figure 4E**). [77, 179-181] For example, guest-host supramolecular chemistry has recently been used to provide hyaluronic acid with reversible shear-thinning and self-healing properties, which allowed excellent printability and structural stability after a secondary photocrosslinking step. [179] One drawback to extrusion-based bioprinting is that cell damage can be caused by induced shear force as viscous bioinks are extruded through a narrow nozzle. [182] However, using a core-shell nozzle unit to present the biopolymer solution and its crosslinker in parallel,

low-viscosity alginate bioinks can be printed into well-defined constructs with high cell viability. [183] Extrusion-based bioprinting can employ multiple nozzles, [184] or multiple channels in a single nozzle, [185] to assemble heterogeneous building blocks. For example, Liu *et al.* developed a nozzle bearing seven individual input channels and showed the assembly of multiple cell types into biomimetic designs. [185] Some advanced extrusion-based techniques have recently emerged, for example, bioprinting on a rotor surface, [77] in supporting baths, [186, 187] or *in situ* at wound sites. [188, 189]

Recently, bioprinting based on light projection has emerged as an alternative strategy for the assembly of living building blocks. This approach generates sheets from a bath of prepolymer solution using a digital micro-mirror device (DMD) [190, 191] or photomask. [192] Stacked 3D constructs are built up by moving the printing stage and changing the light projection pattern. Chen and colleagues pioneered the work of applying digital light processing (DLP) to fabricate cell-laden hydrogel structures. [190, 191] Using cellularized glycidyl methacrylate-hyaluronic acid (GM-HA) and GelMA, they reported the fabrication of prevascularized tissue constructs [191] and a hepatic model with a biomimetic liver lobule pattern. [190] Very recently, Grigoryan *et al.* reported the projection stereolithography bioprinting of cell-laden PEGDA hydrogels with a high resolution (50 μm) by using a biocompatible food dye as an effective photoabsorber. [192] The major advantage of light projection is the speed of assembly: sheets can be generated and stacked within seconds, compared to the much lengthier process of droplet/fiber deposition. There are some challenges to be addressed, however, such as the potential for cell damage caused by the use of high-intensity light and cytotoxic photoabsorbers.

The examples discussed thus far all use supporting biomaterials in the bioinks to simplify the bioprinting process and to protect or support the cells. However, biomaterial-free bioinks have been reported, in which cell-only formulations have been successfully bioprinted. For example, Forgacs and colleagues showed that bioprinting could be used to precisely position cell spheroids onto a layer of printed hydrogel, known as a biopaper. [193] Forgacs and colleagues further investigated the bioprinting of cell spheroids

or cell fibers along with supporting agarose cylinders to form tubular structures bearing double walls, cell heterogeneity, and branched features. [140, 194] Recently, Itoh *et al.* reported the Kenzan method of bioprinting cell spheroids into biomaterial-free tubular tissues, in which spheroids were immobilized by needle arrays during the process of spheroid fusion. [195] More recently, Jeon *et al.* reported the extrusion bioprinting of a cell suspension bioink, with the biomaterial-free fibers supported by depositing the cells into a granular bath of biodegradable and photo-crosslinkable microgels. This method was used to assemble dense cell structures used for cartilage and bone tissue engineering. [196]

5. Remote Assembly of Living Building Blocks

Remote assembly techniques use force fields to interact and manipulate matter in a non-contact fashion, an approach that can be used for modular tissue engineering. While acknowledging that dielectrophoresis [197] and thermal convection [198] have also been used to manipulate living building blocks, here we focus on the three major categories of remote field manipulation: acoustic, magnetic and optical assembly (**Figure 1C**, **Table 2**). [199] Generally, these techniques exploit physical differences between living building blocks and the surrounding medium (*e.g.*, density, compressibility, refractive index, paramagnetism) to exert forces that can be used to remotely assemble different tissue engineering components.

5.1. Acoustic Assembly

Acoustic fields can be used as a non-contact method for manipulating unlabelled, living building blocks. [200, 201] Particles with a difference in compressibility and density to the surrounding medium will experience an acoustic radiation force when placed in an acoustic pressure field. When the acoustic radiation force dominates over competing forces, such as gravity, viscosity or streaming forces, the applied field can be used to move or trap particles. [202] Notably, ultrasound frequencies have wavelengths that can be used to manipulate microscale entities, such as single cells or cell-laden materials. A common

example of single cell manipulation is the use of ultrasound standing waves to remotely aggregate cells into sheets, [203] spheroids, [204-206] pellet tissue cultures, [207] and organoids. [208] In this regard, acoustic fields can be used either as a technology for modular cellular assembly or as a method for controllably fabricating higher-dimensional living building blocks. Acoustic fields can also be used for the assembly of cell-laden biomaterials for tissue engineering. For example, Xu *et al.* used lower frequency ultrasound fields (0.8 – 7.0 kHz) to drive the nodal assembly of cellularized PEG microgels. [121] More recently, Fisher and colleagues have demonstrated two methods employing acoustic holograms for fabricating customized material assemblies. [209, 210] While this approach has not yet been applied to cellularized systems, it offers great potential for the precision assembly of living building blocks for modular tissue engineering.

Hydrogels have been widely used as a method to immobilize acoustically-patterned cell assemblies, enabling long-term tissue culture after removal of the applied field. The first example of this was reported by Garvin *et al.* who showed that acoustic levitation could be used to create flat sheets of endothelial cells in collagen hydrogels, [211] and this approach has since been used to create various vascular tissue models. [212, 213] A similar acoustic levitation method was used by Bouyer *et al.* to generate multilayered assemblies of embryonic stem cell derived neuroprogenitors immobilized in fibrin gels, which were subsequently used for neural tissue engineering. [214] In 2017, two separate groups reported the acoustic assembly of functional cardiomyocytes for cardiac tissue engineering. Naseer *et al.* generated arrays of neonatal rat cardiomyocytes in GelMA, [215] while Serpooshan *et al.* produced assemblies of cardiomyocytes, derived from human induced pluripotent stem cells, within fibrin hydrogels. [216] More recently, Armstrong *et al.* showed that bulk acoustic waves could be used to assemble linear arrays of myoblasts in collagen and GelMA hydrogels, in order to guide cell fusion, enhance myofibrillogenesis and promote mechanical anisotropy during skeletal muscle engineering (**Figure 5A**). [217] An interesting study by Kang *et al.* demonstrated the co-patterning of human adipose derived stem cells and human

vascular endothelial cells into collateral cylindroids. These 3D cell assemblies, immobilized in catechol-conjugated hyaluronic acid hydrogels, promoted enhanced *in vivo* integration and angiogenesis. [218]

5.2. Magnetic Assembly

Magnetic fields can be used to guide the fabrication of living building blocks but also to remotely assemble modular tissue constructs. In either case, the most common approach is to use cells or cellularized materials that are responsive to externally-applied magnetic fields. Biological systems can be magnetized using many different paramagnetic compounds, [219] however, the most commonly used approach is to use superparamagnetic iron oxide nanoparticles (SPIONs). [220, 221] Labelling protocols have been developed that can deliver large quantities of SPIONs to cells, with good biocompatibility profile. [222] However, given the microscale dimensions of cells and cellularized biomaterials, relatively large magnetic fields must be used to exert forces capable of moving the living building blocks against competing forces. Early work on magnetic cell assembly was performed by Ito *et al.*, who used external magnetic fields to assemble sheets of magnetized keratinocytes on nonadherent culture surfaces. [223] This process was used to create assemblies of retinal pigment epithelial cells [224] and skeletal myoblasts, [225, 226] as well as magnetized sheets of endothelial cells, smooth muscle cells, and fibroblasts that could be sequentially assembled *via* magnetic rolling for the engineering of multilayered blood vessels. [227] Other authors have used similar approaches to create multilayered cell sheets of different magnetized cell types, including dental pulp stem cells, bone marrow stem cells, chondrocytes, and endothelial cells. [228]

While uniform magnetic fields are used to assemble cell sheets, the application of nonuniform magnetic fields can be used to create patterned cell assemblies. This approach has been used to pattern endothelial cells onto substrates coated with Matrigel, [229] or onto monolayer sheets of hepatocytes [223] and myoblasts. [230] More recently, Du *et al.* used magnetic microtips to assemble magnetically-labelled embryonic stem cells as a controlled route to forming embryoid bodies. Magnetic fields could then be

used to magnetically stretch the embryoid bodies in order to drive differentiation towards the mesodermal cardiac lineage. [231] A similar approach was used by Adine *et al.*, who used a magnetic pin drive to assemble magnetized human dental pulp stem cells into uniform arrays of spheroids, which were then differentiated into secretory epithelial organoids. [232] A counter strategy to magnetic attraction is the guided assembly of cells and spheroids *via* magnetic levitation, [233] an approach which has been used to engineer vocal fold tissue, [234] adipose tissue, [235] and multicellular spheroid models of the stem cell niche. [236] A more advanced strategy was reported by Tseng *et al.*, in which a magnetized Teflon pen was used to sequentially layer different magnetically-levitated cell sheets. Valvular interstitial cells and valvular endothelial cells were assembled into co-culture models of the aortic valve, [237] while endothelial cells, smooth muscle cells, fibroblasts, and epithelial cells were sequentially layered into multilayered structures resembling the bronchiole. [238] Meanwhile, Tasoglu *et al.* have demonstrated three nanoparticle-free approaches for the magnetic assembly of cellularized materials, using hydrogels crosslinked with Ho^{3+} ions, [239] impregnated with 4-amino-TEMPO radicals (**Figure 5B**) [122] or suspended in a paramagnetic medium. [240]

5.3. Optical Assembly

Optical fields can be used to remotely trigger the formation, cleavage or reorganization of chemical bonds, an approach that has been widely used for additive and subtractive manufacturing, and precision biomaterial modification. [241] Moreover, since light carriers linear and angular momentum, it can also be used to exert forces. This principle is exploited in the operation of optical tweezers, which use highly focused lasers to trap and manoeuvre nano- to microscale matter that bears a refractive index mismatch with the surrounding medium. [242] Holographic optical tweezers have been used for a range of biological applications, including the assembly of cells onto customized arrays. [243, 244] For example, Linnenberger *et al.* assembled linear arrays of myotubes encapsulated in PEG hydrogels for skeletal muscle tissue engineering. [245] Kirkham *et al.* also used holographic optical tweezers to generate a range of different

composite assemblies using embryonic stem cells, mesenchymal stem cells, calvarae cells, microbeads, and electrospun fibers. [246] An issue with using optical tweezers is scalability; it is practically infeasible to manually assemble whole tissue constructs cell-by-cell. However, higher throughput methods have been reported by Akselrod *et al.*, who used time-multiplexed holographic optical traps to manipulate hundreds of cells simultaneously [247] and Mirsaidov *et al.*, who optically trapped and encapsulated cells in a microfluidic channel and then repeated the process to create patterned hydrogel microstructures that could be tiled. [248]

However, a much higher throughput alternative is the use of laser-guided direct writing, in which weakly-focused laser beams are used to radially confine and axially deliver a continuous stream of particles to a non-absorbing surface. [249] This method has been used for the direct writing of many cell types, including embryonic chick neurons [250] and endothelial cells. [251] The latter example used cell-bound microparticles to effectively raise the refractive index of the endothelial cells, moreover, this report also demonstrated how sequential writing could be used to create layer-by-layer endothelial networks. [251, 252] Optical fields have also been used more indirectly to pattern cells using laser-assisted bioprinting, [172] however, these technologies have already been considered in **Section 4.5**. An alternative approach to optical assembly is the use of phototriggered processes that can guide the association of living building blocks. For example, Yüz *et al.* recently showed that cells expressing cryptochrome 2 (CRY2) and the N-terminal of cryptochrome-interacting basic helix-loop-helix protein 1 (CIBN) could be reversibly assembled using optogenetic technology. Specifically, cells expressing CRY2 and CIBN were able to bind each other upon irradiation with blue light (480 nm) and then dissociate when cultured in the dark (**Figure 5C**). [253] In general, light-based assembly offers a high spatial and temporal resolution, guided by fields with precisely tunable wavelength and intensity. However, many applications employ ultraviolet light, high-intensity lasers, and radical photoinitiators; all factors that can negatively impact the viability of cells.

6. Perspectives and Opportunities

6.1. Trends in the Fabrication of Living Building Blocks

Significant progress has been made in the fabrication of living building blocks with enhanced structure or function (**Table 1**). Notably, major advances in synthetic biology have enabled precision cell engineering, which has opened up new opportunities for programmed assembly of cellular units. [10] For example, functionalization of cell surfaces with oligonucleotide sequences has emerged as a highly promising technique to controllably engineer local cell-cell and cell-matrix interactions and leverage control over the tissue assembly process. [20] Such strategies have greatly expanded the capacity of cells as the base unit for modular assembly, an approach that could also be applied to higher-dimensional living building blocks. Indeed, living materials are a new generation of biomaterials composed of living cells that form the material or modulate its functional performance. [254] For example, using engineered commensal bacteria that can produce proteins, cytokines, and growth factors upon external stimuli (*e.g.*, light, enzymes) can be used to elaborate functional ECM in tissue engineering units containing mammalian cells. [255, 256] Indeed, the other major advances in this field have concerned the development of 4D systems, in particular, the emergence of organoids as biologically complex living building blocks. Some recent pioneering works, such as the generation of hybrid cerebral organoid microtissues [135, 136] and centimeter-scale epithelial tubes, [134] have firmly established organoids as viable units for modular tissue engineering. The self-renewing and self-organizing properties of organoids enable more flexible tissue engineering strategies to be employed. For example, an interesting development in this field is the use of vascularized organoids, which offer the opportunity for modular assembly of tissues with pre-formed vascular networks. [57, 58]

A more general trend has been the move towards more automated, controlled and integrated fabrication systems that can produce uniform, reproducible and programmed living building blocks. In general, the fabrication of biomaterial-free cell modules generally proceeds *via* more spontaneous, stochastic

processes relying on variable cellular processes such as adhesion, aggregation, migration and proliferation. These processes can be partially guided by culture conditions, substrate patterning and other methods, however, a greater degree of control can be gained by the inclusion of biomaterials. [53] This approach enables the use of more advanced processing methods; in particular, microfluidics has emerged as a powerful tool for the controlled and programmed fabrication of living building blocks. [14, 16] Looking forward, there is also the opportunity to integrate microfluidics with other technologies, such as acoustics (acoustofluidics [257]), which can enable new methods of living building block fabrication. Moreover, there are many fabrication techniques, particularly those that continuously generate living building blocks, that can be directly integrated with the assembly process. For example, microfluidic devices can act as a cellularized yarn generator for textile process and as a nozzle unit for bioprinting. [71, 72]

6.2. Trends in the Assembly of Living Building Blocks

Each assembly technique has associated advantages and disadvantages (**Table 2**). Although self-assembly is inherently error-correcting, it is challenging to predict the outcome of a spontaneous assembly process when constructing a complex living system. [119] This consideration calls for an improved mechanistic understanding and increased control of self-assembly processes. In this regard, specific molecular recognition allowing coded module assembly is an exciting future direction. The DNA-programmed assembly of cells is a perfect example of this principle, [129] and similar approaches could be used to aid or alter other self-assembly methods, such as cellular fusion and geometric recognition. In reality, while the self-assembly of living building blocks offers an enticing scientific challenge, more complex modular tissue engineering is most likely to be achieved by the directed assembly. Many examples of packing, bundling, and stacking are achieved using manual processing, which introduces a degree of handling error and variability. For the design of translational tissue engineering using directed assembly, it is important to install more automated processing methods. For

example, integrated equipment has been developed for the automated assembly of cell sheets, covering cell culture, tissue harvest, transfer, and stacking, [39] while robotic pick-deposit systems could also be used for modular tissue assembly. [258, 259] Similarly, remote fields offer an attractive option for the controlled assembly of living building blocks. For instance, the use of stable pressure fields exerting a defined acoustic radiation force offers increased reliability compared to manual handling. [202]

Many of the strategies described use only a single form of living building block and recreate only certain features of an engineered tissue. As we strive towards the engineering of more complex tissue structures, it is essential that we develop more flexible assembly strategies. For example, there is a need for integrated methods that can build modular tissues through the co-assembly of different living building blocks. This could enable, for example, the assembly of bulk tissue structures *via* spheroid packing and fusion in combination with the directed assembly of tubular building blocks for vascularization or innervation. However, most methods are restricted to the assembly of a small number of living building blocks with the requisite dimension and form. Thus, it is likely that such approaches will require the careful coordination of different assembly tools that can act across multiple length scales, spanning from single cells units to multidimensional living building blocks. In turn, this will require a better understanding of the interplay between different living building blocks and their respective assembly methods. Additional mechanistic complexity arises from the use of 4D living building blocks, which can lead to dynamic re-organization of the assembled construct. However, if we are able to predict and control these temporal changes in geometry or biology, then we may be able to generate emergent complexity that cannot be realized through static methods of tissue assembly.

6.3. New Opportunities in Bioprinting

The most widely used and versatile methodology in modular tissue assembly is bioprinting, which covers a wide range of living building blocks, including single cells, cell spheroids, cell-laden fibers, cell-laden droplets, and cell-laden sheets (**Table 3**). [174, 195, 260] A major trend in this field is towards generalizable

strategies that can provide a unified approach to printing different composition bioinks. For example, Zhu *et al.* showed that the inclusion of alginate and $CaCl_2$ into a co-axial core and shell, respectively, could enable the printing a variety of different bioinks, including collagen, gelatin, and GelMA. [261] Another generalizable bioprinting strategy was introduced by Ouyang *et al.*, who used an *in-situ* crosslinking strategy to print non-viscous bioink formulations (viscosity <15 mPa s) from various photo-crosslinkable hydrogels (**Figure 4E**). [77] This strategy did not require any additional components to be doped into the bioink, and allowed for standardized bioprinting of different bioink formulations within a tight parameter space. [77] An enduring issue in extrusion bioprinting is the obtainable resolution, which is usually restricted by the fiber size (normally >100 μm). Recently, Lee *et al.* developed a technique known as freeform reversible embedding of suspended hydrogels (FRESH), which used a bath of gelatin microparticles to support the 3D bioprinting of fine fibers with diameters down to 20 μm (**Figure 6A**). [186] This approach, and other matrix-supported methodologies, [187, 262] have attracted huge attention for modular tissue assembly.

An impressive take on this methodology was recently reported by Skylar-Scott *et al.*, who used a packed bed of hundreds of thousands of living organoids that acted not only as the bulk tissue matrix but also as the supporting material for 3D bioprinting of sacrificial bioinks (**Figure 6B**). [263] Although this method could be used to assemble various complex tissue features, the authors demonstrated applicability in assembling tissues with templated vascular networks. Indeed, bioprinting seems to be uniquely suited for the modular assembly of vascularized networks, and there have been many recent reports detailing new vascularization strategies. In particular, many of these methods use a multistep methodology in which sacrificial printed templates are used to create channels that are then seeded with endothelial cells. [263-265] Recently, Ouyang *et al.* introduced a new method in which a sacrificial bioink laden with endothelial cells could be printed alongside a matrix bioink to form a void-free structure. This strategy allowed *in-situ* endothelialization on the walls of the newly-formed channels, an approach that enabled increased

uniformity, efficiency, and control when compared to post-seeding approaches (**Figure 6C**). [266] Other studies have focused on the creation of vascular networks with a multiscale geometry that is more faithful to natural tissue. [186, 262] These different methods will be essential for building complex structures that can efficiently perfuse large tissue constructs and integrate with the host vascular network.

6.4. Concluding Remarks

Modular assembly of living building blocks has shown great potential in engineering complex tissues, offering inherent control over microscale tissue features. Recent advances have greatly expanded the palette of living building blocks, from zero-dimensional units (native or engineered single cells) to 4D structures that undergo temporal re-organization (organoids or shape-changing materials). There has also been rapid progress in the different assembly techniques, including advances in programmed self-assembly, automated directed assembly, and noncontact remote assembly. Although a number of challenges remain, we anticipate that the swathe of new enabling technologies presented in this Progress Report will hasten progress towards the modular assembly and engineering of more complex tissue targets.

Acknowledgments

The authors acknowledge help from Li Li for the schematic drawings in Figure 1. L.O., M.S.S. and M.M.S. acknowledge the financial support from Engineering and Physical Sciences Research Council (EPSRC) Programme Grant “Engineering growth factor microenvironments - a new therapeutic paradigm for regenerative medicine” (EP/P001114/1). J.P.K.A. acknowledges support from the Medical Research Council (MRC) (MR/S00551X/1). M.S.S. and M.M.S. acknowledge support from a grant from the UK Regenerative Medicine Platform “Acellular / Smart Materials – 3D Architecture” (MR/R015651/1). M.M.S. acknowledges support from the Wellcome Trust Senior Investigator Award (098411/Z/12/Z).

Peer reviewed version of the manuscript published in final form in Advanced Functional Materials (2020)

Received: ((will be filled in by the editorial staff))

Revised: ((will be filled in by the editorial staff))

Published online: ((will be filled in by the editorial staff))

References

[1] E. S. Place, N. D. Evans, M. M. Stevens, *Nat Mater* **2009**, *8*, 457.
[2] R. H. Harrison, J. P. St-Pierre, M. M. Stevens, *Tissue Eng Part B Rev* **2014**, *20*, 1.
[3] J. P. K. Armstrong, M. M. Stevens, *Tissue Eng Part A* **2019**, *25*, 688.
[4] S. L. Wu, X. M. Liu, K. W. K. Yeung, C. S. Liu, X. J. Yang, *Mater Sci Eng R Rep* **2014**, *80*, 1.
[5] A. Atala, F. K. Kasper, A. G. Mikos, *Sci Transl Med* **2012**, *4*, 160rv12.
[6] E. C. Novosel, C. Kleinhans, P. J. Kluger, *Adv Drug Deliv Rev* **2011**, *63*, 300.
[7] J. Laurent, G. Blin, F. Chatelain, V. Vanneaux, A. Fuchs, J. Larghero, M. Thery, *Nat Biomed Eng* **2017**, *1*, 939.
[8] J. W. Nichol, A. Khademhosseini, *Soft Matter* **2009**, *5*, 1312.
[9] D. L. Elbert, *Curr Opin Biotechnol* **2011**, *22*, 674.
[10] J. S. Liu, Z. J. Gartner, *Trends Cell Biol* **2012**, *22*, 683.
[11] S. Guven, P. Chen, F. Inci, S. Tasoglu, B. Erkmen, U. Demirci, *Trends Biotechnol* **2015**, *33*, 269.
[12] A. Tamayol, M. Akbari, N. Annabi, A. Paul, A. Khademhosseini, D. Juncker, *Biotechnol Adv* **2013**, *31*, 669.
[13] H. Onoe, S. Takeuchi, *Drug Discov Today* **2015**, *20*, 236.
[14] Y. Morimoto, A. Y. Hsiao, S. Takeuchi, *Adv Drug Deliv Rev* **2015**, *95*, 29.
[15] G. H. Lee, J. S. Lee, X. H. Wang, S. H. Lee, *Adv Funct Mater* **2016**, *5*, 56.
[16] M. H. Nie, S. Takeuchi, *Biofabrication* **2018**, *10*, 044103.
[17] R. D. Pedde, B. Mirani, A. Navaei, T. Styan, S. Wong, M. Mehrali, A. Thakur, N. K. Mohtaram, A. Bayati, A. Dolatshahi-Pirouz, M. Nikkhah, S. M. Willerth, M. Akbari, *Adv Mater* **2017**, *29*, 1606061.
[18] L. Moroni, J. A. Burdick, C. Highley, S. J. Lee, Y. Morimoto, S. Takeuchi, J. J. Yoo, *Nat Rev Mater* **2018**, *3*, 21.
[19] M. Jinek, K. Chylinski, I. Fonfara, M. Hauer, J. A. Doudna, E. Charpentier, *Science* **2012**, *337*, 816.
[20] Z. J. Gartner, C. R. Bertozzi, *Proc Natl Acad Sci U S A* **2009**, *106*, 4606.
[21] J. P. K. Armstrong, A. W. Perriman, *Exp Biol Med* **2016**, *241*, 1098.
[22] R. Sackstein, J. S. Merzaban, D. W. Cain, N. M. Dagia, J. A. Spencer, C. P. Lin, R. Wohlgemuth, *Nat Med* **2008**, *14*, 181.
[23] D. Sarkar, P. K. Vemula, G. S. Teo, D. Spelke, R. Karnik, Y. Wee le, J. M. Karp, *Bioconjug Chem* **2008**, *19*, 2105.
[24] M. T. Stephan, J. J. Moon, S. H. Um, A. Bershteyn, D. J. Irvine, *Nat Med* **2010**, *16*, 1035.
[25] E. Saxon, C. R. Bertozzi, *Science* **2000**, *287*, 2007.
[26] S. C. Carreira, J. P. K. Armstrong, A. M. Seddon, A. W. Perriman, R. Hartley-Davies, W. Schwarzacher, *Nanoscale* **2016**, *8*, 7474.
[27] B. R. McNaughton, J. J. Cronican, D. B. Thompson, D. R. Liu, *Proc Natl Acad Sci U S A* **2009**, *106*, 6111.
[28] R. S. McHugh, S. N. Ahmed, Y. C. Wang, K. W. Sell, P. Selvaraj, *Proc Natl Acad Sci U S A* **1995**, *92*, 8059.
[29] J. P. K. Armstrong, R. Shakur, J. P. Horne, S. C. Dickinson, C. T. Armstrong, K. Lau, J. Kadiwala, R. Lowe, A. Seddon, S. Mann, J. L. R. Anderson, A. W. Perriman, A. P. Hollander, *Nat Commun* **2015**, *6*, 7405.
[30] G. Shi, R. Mukthavaram, S. Kesari, D. Simberg, *Adv Healthc Mater* **2014**, *3*, 142.
[31] R. C. Deller, T. Richardson, R. Richardson, L. Bevan, I. Zampetakis, F. Scarpa, A. W. Perriman, *Nat Commun* **2019**, *10*, 1887.
[32] E. Gantumur, M. Kimura, M. Taya, M. Horie, N. M., S. Sakai, *Biofabrication* **2020**, *12*, 011001.
[33] K. Mubyana, D. T. Corr, *Tissue Eng Part A* **2018**.
[34] A. Akkouch, Y. Yu, I. T. Ozbolat, *Biofabrication* **2015**, *7*, 031002.
[35] Y. Yu, K. K. Moncal, J. Li, W. Peng, I. Rivero, J. A. Martin, I. Ozbolat, *Sci Rep* **2016**, *6*, 28714.
[36] N. Yamada, T. Okano, H. Sakai, F. Karikusa, Y. Sawasaki, Y. Sakurai, *Macromol Rapid Commun* **1990**, *11*, 571.
[37] T. Okano, N. Yamada, M. Okuhara, H. Sakai, Y. Sakurai, *Biomaterials* **1995**, *16*, 297.
[38] K. Matsuura, M. Wada, T. Shimizu, Y. Haraguchi, F. Sato, K. Sugiyama, K. Konishi, Y. Shiba, H. Ichikawa, A. Tachibana, U. Ikeda, M. Yamato, N. Hagiwara, T. Okano, *Biochem Biophys Res Commun* **2012**, *425*, 321.
[39] T. Owaki, T. Shimizu, M. Yamato, T. Okano, *Biotechnol J* **2014**, *9*, 904.
[40] N. Matsuda, T. Shimizu, M. Yamato, T. Okano, *Adv Mater* **2007**, *19*, 3089.
[41] J. Kobayashi, A. Kikuchi, T. Aoyagi, T. Okano, *J Biomed Mater Res A* **2019**, *107*, 955.
[42] N. G. Rim, A. Yih, P. Hsi, Y. J. Wang, Y. H. Zhang, J. Y. Wong, *Biomaterials* **2018**, *181*, 126.
[43] C. Liu, Y. Zhou, M. Sun, Q. Li, L. Dong, L. Ma, K. Cheng, W. Weng, M. Yu, H. Wang, *ACS Appl Mater Interfaces* **2017**, *9*, 36513.

[44] P. R. Baraniak, T. C. McDevitt, *Cell Tissue Res* **2012**, *347,* 701.
[45] S. L. Nyberg, J. Hardin, B. Amiot, U. A. Argikar, R. P. Remmel, P. Rinaldo, *Liver Transpl* **2005**, *11,* 901.
[46] H. Ota, R. Yamamoto, K. Deguchi, Y. Tanaka, Y. Kazoe, Y. Sato, N. Miki, *Sens Actuators B Chem* **2010**, *147,* 359.
[47] M. A. Phelan, A. L. Gianforcaro, J. A. Gerstenhaber, P. I. Lelkes, *Tissue Eng Part C Methods* **2019**, *25,* 479.
[48] O. Frey, P. M. Misun, D. A. Fluri, J. G. Hengstler, A. Hierlemann, *Nat Commun* **2014**, *5,* 4250.
[49] L. Ouyang, R. Yao, S. Mao, X. Chen, J. Na, W. Sun, *Biofabrication* **2015**, *7,* 044101.
[50] Y. Zhao, R. Yao, L. Ouyang, H. Ding, T. Zhang, K. Zhang, S. Cheng, W. Sun, *Biofabrication* **2014**, *6,* 035001.
[51] L. Ouyang, R. Yao, X. Chen, J. Na, W. Sun, *Biofabrication* **2015**, *7,* 015010.
[52] E. Wang, D. Wang, A. Geng, R. Seo, X. Gong, *Biomaterials* **2017**, *143,* 57.
[53] J. A. Brassard, M. P. Lutolf, *Cell Stem Cell* **2019**, *24,* 860.
[54] S. L. Giandomenico, S. B. Mierau, G. M. Gibbons, L. M. D. Wenger, L. Masullo, T. Sit, M. Sutcliffe, J. Boulanger, M. Tripodi, E. Derivery, O. Paulsen, A. Lakatos, M. A. Lancaster, *Nat Neuroscience* **2019**, *22,* 669.
[55] M. A. Lancaster, N. S. Corsini, S. Wolfinger, E. H. Gustafson, A. W. Phillips, T. R. Burkard, T. Otani, F. J. Livesey, J. A. Knoblich, *Nat Biotechnol* **2017**, *35,* 659.
[56] N. Gjorevski, N. Sachs, A. Manfrin, S. Giger, M. E. Bragina, P. Ordonez-Moran, H. Clevers, M. P. Lutolf, *Nature* **2016**, *539,* 560.
[57] K. A. Homan, N. Gupta, K. T. Kroll, D. B. Kolesky, M. Skylar-Scott, T. Miyoshi, D. Mau, M. T. Valerius, T. Ferrante, J. V. Bonventre, J. A. Lewis, R. Morizane, *Nat Methods* **2019**, *16,* 255.
[58] T. Takebe, M. Enomura, E. Yoshizawa, M. Kimura, H. Koike, Y. Ueno, T. Matsuzaki, T. Yamazaki, T. Toyohara, K. Osafune, H. Nakauchi, H. Y. Yoshikawa, H. Taniguchi, *Cell Stem Cell* **2015**, *16,* 556.
[59] T. Kamperman, M. Karperien, S. Le Gac, J. Leijten, *Trends Biotechnol* **2018**, *36,* 850.
[60] E. W. M. Kemna, R. M. Schoeman, F. Wolbers, I. Vermes, D. A. Weitz, A. van den Berg, *Lab Chip* **2012**, *12,* 2881.
[61] S. Ma, M. Natoli, X. Liu, M. Neubauer, F. M. Watt, A. Fery, W. T. S. Huck, *J Mater Chem B* **2013**, *8,* 5128.
[62] T. Kamperman, S. Henke, C. W. Visser, M. Karperien, J. Leijten, *Small* **2017**, *13,* 1603711.
[63] T. Kamperman, S. Henke, A. van den Berg, S. R. Shin, A. Tamayol, A. Khademhosseini, M. Karperien, J. Leijten, *Adv Healthc Mater* **2017**, *6,* 1600913.
[64] A. S. Mao, J. W. Shin, S. Utech, H. Wang, O. Uzun, W. Li, M. Cooper, Y. Hu, L. Zhang, D. A. Weitz, D. J. Mooney, *Nat Mater* **2017**, *16,* 236.
[65] P. S. Lienemann, T. Rossow, A. S. Mao, Q. Vallmajo-Martin, M. Ehrbar, D. J. Mooney, *Lab Chip* **2017**, *17,* 727.
[66] D. Neal, M. S. Sakar, L. L. S. Ong, H. H. Asada, *Lab Chip* **2014**, *14,* 1907.
[67] Y. Yu, W. Wei, Y. Wang, C. Xu, Y. Guo, J. Qin, *Adv Mater* **2016**, *28,* 6649.
[68] E. Kang, G. S. Jeong, Y. Y. Choi, K. H. Lee, A. Khademhosseini, S. H. Lee, *Nat Mater* **2011**, *10,* 877.
[69] Y. Cheng, F. Zheng, J. Lu, L. Shang, Z. Xie, Y. Zhao, Y. Chen, Z. Gu, *Adv Mater* **2014**, *26,* 5184.
[70] Y. Yu, L. Shang, J. Guo, J. Wang, Y. Zhao, *Nat Protoc* **2018**, *13,* 2557.
[71] H. Onoe, T. Okitsu, A. Itou, M. Kato-Negishi, R. Gojo, D. Kiriya, K. Sato, S. Miura, S. Iwanaga, K. Kuribayashi-Shigetomi, Y. T. Matsunaga, Y. Shimoyama, S. Takeuchi, *Nat Mater* **2013**, *12,* 584.
[72] M. A. Daniele, S. H. North, J. Naciri, P. B. Howell, S. H. Foulger, F. S. Ligler, A. A. Adams, *Adv Funct Mater* **2013**, *23,* 698.
[73] M. Khanmohammadi, S. Sakai, M. Taya, *Int J Biol Macromol* **2017**, *104,* 204.
[74] Y. Morimoto, M. Kiyosawa, S. Takeuchi, *Sens Actuators B Chem* **2018**, *274,* 491.
[75] S. M. Mihaila, E. G. Popa, R. L. Reis, A. P. Marques, M. E. Gomes, *Biomacromolecules* **2014**, *15,* 2849.
[76] Y. H. Li, C. T. Poon, M. X. Li, T. J. Lu, B. Pingguan-Murphy, F. Xu, *Adv Funct Mater* **2015**, *25,* 5999.
[77] L. Ouyang, C. B. Highley, W. Sun, J. A. Burdick, *Adv Mater* **2017**, *29,* 1604983.
[78] S. Zhang, M. A. Greenfield, A. Mata, L. C. Palmer, R. Bitton, J. R. Mantei, C. Aparicio, M. O. de la Cruz, S. I. Stupp, *Nat Mater* **2010**, *9,* 594.
[79] S. L. Sampson, L. Saraiva, K. Gustafsson, S. N. Jayasinghe, B. D. Robertson, *Small* **2014**, *10,* 78.
[80] M. Yeo, G. H. Kim, *Small* **2018**, *14,* 1803491.
[81] E. Nam, W. C. Lee, S. Takeuchi, *Macromol Biosci* **2016**, *16,* 995.
[82] Y. Yajima, M. Yamada, R. Utoh, M. Seki, *ACS Biomater Sci Eng* **2017**, *3,* 2144.
[83] W. Bian, B. Liau, N. Badie, N. Bursac, *Nat Protoc* **2009**, *4,* 1522.

[84] D. Zhang, I. Y. Shadrin, J. Lam, H. Q. Xian, H. R. Snodgrass, N. Bursac, *Biomaterials* **2013**, *34*, 5813.
[85] J. Son, C. Y. Bae, J. K. Park, *Biotechnol J* **2016**, *11*, 585.
[86] L. Leng, A. McAllister, B. Zhang, M. Radisic, A. Gunther, *Adv Mater* **2012**, *24*, 3650.
[87] A. Kobayashi, K. Yamakoshi, Y. Yajima, R. Utoh, M. Yamada, M. Seki, *J Biosci Bioeng* **2013**, *116*, 761.
[88] X. Wang, Q. L. Jiao, S. J. Zhang, Z. Y. Ye, Y. Zhou, W. S. Tan, *Biotechnol J* **2014**, *9*, 1425.
[89] A. Leferink, D. Schipper, E. Arts, E. Vrij, N. Rivron, M. Karperien, K. Mittmann, C. van Blitterswijk, L. Moroni, R. Truckenmuller, *Adv Mater* **2014**, *26*, 2592.
[90] W. Jiang, M. Li, Z. Chen, K. W. Leong, *Lab Chip* **2016**, *16*, 4482.
[91] H. F. Chan, Y. Zhang, K. W. Leong, *Small* **2016**, *12*, 2720.
[92] H. F. Chan, Y. Zhang, Y. P. Ho, Y. L. Chiu, Y. Jung, K. W. Leong, *Sci Rep* **2013**, *3*, 3462.
[93] A. Kumachev, J. Greener, E. Tumarkin, E. Eiser, P. W. Zandstra, E. Kumacheva, *Biomaterials* **2011**, *32*, 1477.
[94] J. Yeh, Y. Ling, J. M. Karp, J. Gantz, A. Chandawarkar, G. Eng, J. Blumling, 3rd, R. Langer, A. Khademhosseini, *Biomaterials* **2006**, *27*, 5391.
[95] H. Wang, H. Liu, H. Liu, W. Su, W. Chen, J. Qin, *Adv Mater Technol* **2019**, *4*, 1800632.
[96] D. M. Headen, G. Aubry, H. Lu, A. J. Garcia, *Adv Mater* **2014**, *26*, 3003.
[97] M. G. A. Mohamed, S. Kheiri, S. Islam, H. Kumar, A. Yang, K. Kim, *Lab Chip* **2019**, *19*, 1621.
[98] A. C. Mendes, E. T. Baran, P. Lisboa, R. L. Reis, H. S. Azevedo, *Biomacromolecules* **2012**, *13*, 4039.
[99] D. S. Ferreira, R. L. Reis, H. S. Azevedo, *Soft Matter* **2013**, *9*, 9237.
[100] J. S. Lee, Y. H. Roh, Y. S. Choi, Y. Jin, E. J. Jeon, K. W. Bong, S. W. Cho, *Adv Funct Mater* **2019**, *29*, 1807803.
[101] C. H. Choi, H. N. Wang, H. Lee, J. H. Kim, L. Y. Zhang, A. Mao, D. J. Mooney, D. A. Weitz, *Lab Chip* **2016**, *16*, 1549.
[102] R. Yao, R. Zhang, J. Luan, F. Lin, *Biofabrication* **2012**, *4*, 025007.
[103] S. J. Xin, D. Chimene, J. E. Garza, A. K. Gaharwar, D. L. Alge, *Biomater Sci* **2019**, *7*, 1179.
[104] H. Gudapati, M. Dey, I. Ozbolat, *Biomaterials* **2016**, *102*, 20.
[105] A. Shahin-Shamsabadi, P. R. Selvaganapathy, *Acta Biomater* **2019**, *92*, 172.
[106] Y. Du, E. Lo, S. Ali, A. Khademhosseini, *Proc Natl Acad Sci U S A* **2008**, *105*, 9522.
[107] H. P. Wang, J. Cui, Z. Q. Zheng, Q. Shi, T. Sun, X. M. Liu, Q. Huang, T. Fukuda, *ACS Appl Mater Interfaces* **2017**, *9*, 41669.
[108] J. Cui, H. P. Wang, Z. Q. Zheng, Q. Shi, T. Sun, Q. Huang, T. Fukuda, *Biofabrication* **2019**, *11*, 015016.
[109] Z. Q. Zheng, H. P. Wang, J. N. Li, Q. Shi, J. Cui, T. Sun, Q. Huang, T. Fukuda, *ACS Appl Mater Interfaces* **2019**, *11*, 22950.
[110] G. Stoychev, N. Puretskiy, L. Ionov, *Soft Matter* **2011**, *7*, 3277.
[111] M. Jamal, S. S. Kadam, R. Xiao, F. Jivan, T. M. Onn, R. Fernandes, T. D. Nguyen, D. H. Gracias, *Adv Healthc Mater* **2013**, *2*, 1142.
[112] V. Stroganov, J. Pant, G. Stoychev, A. Janke, D. Jehnichen, A. Fery, H. Handa, L. Ionov, *Adv Funct Mater* **2018**, *28*, 1706248.
[113] A. Kirillova, R. Maxson, G. Stoychev, C. T. Gomillion, L. Ionov, *Adv Mater* **2017**, *29*, 1703443.
[114] K. Kuribayashi-Shigetomi, H. Onoe, S. Takeuchi, *PLoS One* **2012**, *7*, e51085.
[115] Y. Du, M. Ghodousi, E. Lo, M. K. Vidula, O. Emiroglu, A. Khademhosseini, *Biotechnol Bioeng* **2010**, *105*, 655.
[116] B. Zamanian, M. Masaeli, J. W. Nichol, M. Khabiry, M. J. Hancock, H. Bae, A. Khademhosseini, *Small* **2010**, *6*, 937.
[117] F. Yanagawa, H. Kaji, Y. H. Jang, H. Bae, D. Yanan, J. Fukuda, H. Qi, A. Khademhosseini, *J Biomed Mater Res A* **2011**, *97*, 93.
[118] D. Wei, W. Q. Xiao, J. Sun, M. L. Zhong, L. K. Guo, H. S. Fan, X. D. Zhang, *J Mater Chem B* **2015**, *3*, 2753.
[119] N. Bowden, A. Terfort, J. Carbeck, G. M. Whitesides, *Science* **1997**, *276*, 233.
[120] G. Eng, B. W. Lee, H. Parsa, C. D. Chin, J. Schneider, G. Linkov, S. K. Sia, G. Vunjak-Novakovic, *Proc Natl Acad Sci U S A* **2013**, *110*, 4551.
[121] F. Xu, T. D. Finley, M. Turkaydin, Y. R. Sung, U. A. Gurkan, A. S. Yavuz, R. O. Guldiken, U. Demirci, *Biomaterials* **2011**, *32*, 7847.
[122] S. Tasoglu, C. H. Yu, H. I. Gungordu, S. Guven, T. Vural, U. Demirci, *Nat Commun* **2014**, *5*, 4702.
[123] D. Dutta, A. Pulsipher, W. Luo, M. N. Yousaf, *J Am Chem Soc* **2011**, *133*, 8704.
[124] P. J. O'Brien, W. Luo, D. Rogozhnikov, J. Chen, M. N. Yousaf, *Bioconjug Chem* **2015**, *26*, 1939.

[125] H. Koo, M. Choi, E. Kim, S. K. Hahn, R. Weissleder, S. H. Yun, *Small* **2015**, *11*, 6458.
[126] B. Liu, Y. Liu, A. K. Lewis, W. Shen, *Biomaterials* **2010**, *31*, 4918.
[127] M. H. Yao, J. Yang, J. T. Song, D. H. Zhao, M. S. Du, Y. D. Zhao, B. Liu, *Chem Commun (Camb)* **2014**, *50*, 9405.
[128] C. Y. Li, D. K. Wood, C. M. Hsu, S. N. Bhatia, *Lab Chip* **2011**, *11*, 2967.
[129] M. E. Todhunter, N. Y. Jee, A. J. Hughes, M. C. Coyle, A. Cerchiari, J. Farlow, J. C. Garbe, M. A. LaBarge, T. A. Desai, Z. J. Gartner, *Nat Methods* **2015**, *12*, 975.
[130] B. D. Hoffman, A. S. Yap, *Trends Cell Biol* **2015**, *25*, 803.
[131] D. M. Dean, J. R. Morgan, *Tissue Eng Part A* **2008**, *14*, 1989.
[132] A. P. Rago, D. M. Dean, J. R. Morgan, *Biotechnol Bioeng* **2009**, *102*, 1231.
[133] M. Kato-Negishi, H. Onoe, A. Ito, S. Takeuchi, *Adv Healthc Mater* **2017**, *6*, 1700143.
[134] N. Sachs, Y. Tsukamoto, P. Kujala, P. J. Peters, H. Clevers, *Development* **2017**, *144*, 1107.
[135] Y. Xiang, Y. Tanaka, B. Patterson, Y. J. Kang, G. Govindaiah, N. Roselaar, B. Cakir, K. Y. Kim, A. P. Lombroso, S. M. Hwang, M. Zhong, E. G. Stanley, A. G. Elefanty, J. R. Naegele, S. H. Lee, S. M. Weissman, I. H. Park, *Cell Stem Cell* **2017**, *21*, 383.
[136] J. A. Bagley, D. Reumann, S. Bian, J. Levi-Strauss, J. A. Knoblich, *Nat Methods* **2017**, *14*, 743.
[137] F. Birey, J. Andersen, C. D. Makinson, S. Islam, W. Wei, N. Huber, H. C. Fan, K. R. C. Metzler, G. Panagiotakos, N. Thom, N. A. O'Rourke, L. M. Steinmetz, J. A. Bernstein, J. Hallmayer, J. R. Huguenard, S. P. Pasca, *Nature* **2017**, *545*, 54.
[138] A. P. McGuigan, M. V. Sefton, *Proc Natl Acad Sci U S A* **2006**, *103*, 11461.
[139] A. P. McGuigan, B. Leung, M. V. Sefton, *Nat Protocols* **2006**, *1*, 2963.
[140] C. Norotte, F. S. Marga, L. E. Niklason, G. Forgacs, *Biomaterials* **2009**, *30*, 5910.
[141] E. Vrij, J. Rouwkema, V. LaPointe, C. van Blitterswijk, R. Truckenmuller, N. Rivron, *Adv Mater* **2016**, *28*, 4032.
[142] H. Lin, Q. Li, Y. Lei, *Biofabrication* **2017**, *9*, 025007.
[143] O. F. Khan, D. N. Voice, B. M. Leung, M. V. Sefton, *Adv Healthc Mater* **2015**, *4*, 113.
[144] A. M. Leferink, M. P. Tibbe, E. G. B. M. Bossink, L. E. Heus, H. Vossen, A. Berg, L. Moroni, R. Truckenbrodt, *Materials today Bio* **2019**, *4*, 100025.
[145] Y. Pang, S. Sutoko, Y. Horimoto, D. Weng, K. Montagne, K. Komori, K. Takano, R. Shirakashi, M. Anzai, T. Niino, Y. Sakai, *Biochem Eng J* **2019**, *149*.
[146] M. F. Leong, J. K. Toh, C. Du, K. Narayanan, H. F. Lu, T. C. Lim, A. C. Wan, J. Y. Ying, *Nat Commun* **2013**, *4*, 2353.
[147] Y. Yajima, C. N. Lee, M. Yamada, R. Utoh, M. Seki, *J Biosci Bioeng* **2018**, *126*, 111.
[148] P. Patil, J. M. Szymanski, A. W. Feinberg, *Adv Mater Technol* **2016**, *1*, 1600003.
[149] Y. Haraguchi, T. Shimizu, T. Sasagawa, H. Sekine, K. Sakaguchi, T. Kikuchi, W. Sekine, S. Sekiya, M. Yamato, M. Umezu, T. Okano, *Nat Protoc* **2012**, *7*, 850.
[150] M. S. Kim, B. Lee, H. N. Kim, S. Bang, H. S. Yang, S. M. Kang, K. Y. Suh, S. H. Park, N. L. Jeon, *Biofabrication* **2017**, *9*, 015029.
[151] S. Hong, B. Y. Jung, C. Hwang, *Tissue Eng Regen Med* **2017**, *14*, 371.
[152] W. H. Zimmermann, I. Melnychenko, G. Wasmeier, M. Didie, H. Naito, U. Nixdorff, A. Hess, L. Budinsky, K. Brune, B. Michaelis, S. Dhein, A. Schwoerer, H. Ehmke, T. Eschenhagen, *Nat Med* **2006**, *12*, 452.
[153] R. Derda, A. Laromaine, A. Mammoto, S. K. Tang, T. Mammoto, D. E. Ingber, G. M. Whitesides, *Proc Natl Acad Sci U S A* **2009**, *106*, 18457.
[154] R. Derda, S. K. Tang, A. Laromaine, B. Mosadegh, E. Hong, M. Mwangi, A. Mammoto, D. E. Ingber, G. M. Whitesides, *PLoS One* **2011**, *6*, e18940.
[155] B. Mosadegh, B. E. Dabiri, M. R. Lockett, R. Derda, P. Campbell, K. K. Parker, G. M. Whitesides, *Adv Healthc Mater* **2014**, *3*, 1036.
[156] R. Gauvin, T. Ahsan, D. Larouche, P. Levesque, J. Dube, F. A. Auger, R. M. Nerem, L. Germain, *Tissue Eng Part A* **2010**, *16*, 1737.
[157] R. Othman, G. E. Morris, D. A. Shah, S. Hall, G. Hall, K. Wells, K. M. Shakesheff, J. E. Dixon, *Biofabrication* **2015**, *7*, 025003.
[158] L. Ouyang, J. A. Burdick, W. Sun, *ACS Appl Mater Interfaces* **2018**, *10*, 12424.
[159] F. T. Moutos, L. E. Freed, F. Guilak, *Nat Mater* **2007**, *6*, 162.

[160] I. C. Liao, F. T. Moutos, B. T. Estes, X. Zhao, F. Guilak, *Adv Funct Mater* **2013**, *23*, 5833.
[161] M. Younesi, A. Islam, V. Kishore, J. M. Anderson, O. Akkus, *Adv Funct Mater* **2014**, *24*, 5762.
[162] I. Calejo, R. Costa-Almeida, R. L. Reis, M. E. Gomes, *Adv Funct Mater* **2019**, *8*, 1900200.
[163] M. Akbari, A. Tamayol, S. Bagherifard, L. Serex, P. Mostafalu, N. Faramarzi, M. H. Mohammadi, A. Khademhosseini, *Adv Healthc Mater* **2016**, *5*, 751.
[164] M. Akbari, A. Tamayol, V. Laforte, N. Annabi, A. H. Najafabadi, A. Khademhosseini, D. Juncker, *Adv Funct Mater* **2014**, *24*, 4060.
[165] R. Costa-Almeida, R. M. A. Domingues, A. Fallahi, H. Avci, I. K. Yazdi, M. Akbari, R. L. Reis, A. Tamayol, M. E. Gomes, A. Khademhosseini, *J Tissue Eng Regen Med* **2018**, *12*, 1039.
[166] J. Groll, T. Boland, T. Blunk, J. A. Burdick, D. W. Cho, P. D. Dalton, B. Derby, G. Forgacs, Q. Li, V. A. Mironov, L. Moroni, M. Nakamura, W. Shu, S. Takeuchi, G. Vozzi, T. B. Woodfield, T. Xu, J. J. Yoo, J. Malda, *Biofabrication* **2016**, *8*, 013001.
[167] L. Moroni, T. Boland, J. A. Burdick, C. De Maria, B. Derby, G. Forgacs, J. Groll, Q. Li, J. Malda, V. A. Mironov, C. Mota, M. Nakamura, W. Shu, S. Takeuchi, T. B. F. Woodfield, T. Xu, J. J. Yoo, G. Vozzi, *Trends Biotechnol* **2018**, *36*, 384.
[168] T. Xu, J. Jin, C. Gregory, J. J. Hickman, T. Boland, *Biomaterials* **2005**, *26*, 93.
[169] T. Xu, C. A. Gregory, P. Molnar, X. Cui, S. Jalota, S. B. Bhaduri, T. Boland, *Biomaterials* **2006**, *27*, 3580.
[170] C. L. Hedegaard, E. C. Collin, C. Redondo-Comez, L. T. H. Nguyen, K. W. Ng, C.-P. A. A., C.-P. J. R., A. Mata, *Adv Funct Mater* **2018**, *28*, 1703716.
[171] A. Faulkner-Jones, C. Fyfe, D. J. Cornelissen, J. Gardner, J. King, A. Courtney, W. M. Shu, *Biofabrication* **2015**, *7*, 044102.
[172] F. Guillemot, A. Souquet, S. Catros, B. Guillotin, *Nanomedicine (Lond)* **2010**, *5*, 507.
[173] U. Demirci, G. Montesano, *Lab Chip* **2007**, *7*, 1139.
[174] S. Mi, S. Yang, T. Liu, Z. Du, Y. Xu, B. Li, W. Sun, *IEEE Trans Biomed Eng* **2019**, *66*, 2512.
[175] T. liu, Y. Pang, Z. Zhou, R. Yao, W. Sun, *Acta Biomater* **2019**, *95*, 245.
[176] K. Witte, A. Rodrigo-Navarro, M. Salmeron-Sanchez, *Materials Today Bio* **2019**, *2*, 100011.
[177] A. D. Graham, S. N. Olof, M. J. Burke, J. P. K. Armstrong, E. A. Mikhailova, J. G. Nicholson, S. J. Box, F. G. Szele, A. W. Perriman, H. Bayley, *Sci Rep* **2017**, *7*, 7004.
[178] J. Malda, J. Visser, F. P. Melchels, T. Jungst, W. E. Hennink, W. J. Dhert, J. Groll, D. W. Hutmacher, *Adv Mater* **2013**, *25*, 5011.
[179] L. Ouyang, C. B. Highley, C. B. Rodell, W. Sun, J. A. Burdick, *ACS Biomater Sci Eng* **2016**, *2*, 1743.
[180] J. P. K. Armstrong, M. Burke, B. M. Carter, S. A. Davis, A. W. Perriman, *Adv Funct Mater* **2016**, *5*, 1724.
[181] L. Ouyang, *Study on Microextrusion-based 3D Bioprinting and Bioink Crosslinking Mechanisms*, Springer, Singapore, **2019**, p. 25.
[182] L. Ouyang, R. Yao, Y. Zhao, W. Sun, *Biofabrication* **2016**, *8*, 035020.
[183] C. Colosi, S. R. Shin, V. Manoharan, S. Massa, M. Costantini, A. Barbetta, M. R. Dokmeci, M. Dentini, A. Khademhosseini, *Adv Mater* **2016**, *28*, 677.
[184] S. Khalil, J. Nam, W. Sun, *Rapid Prototyp J* **2005**, *11*, 9.
[185] W. Liu, Y. S. Zhang, M. A. Heinrich, F. De Ferrari, H. L. Jang, S. M. Bakht, M. M. Alvarez, J. Yang, Y. C. Li, G. Trujillo-de Santiago, A. K. Miri, K. Zhu, P. Khoshakhlagh, G. Prakash, H. Cheng, X. Guan, Z. Zhong, J. Ju, G. H. Zhu, X. Jin, S. R. Shin, M. R. Dokmeci, A. Khademhosseini, *Adv Mater* **2017**, *29*, 1604630.
[186] A. Lee, A. R. Hudson, D. J. Shiwarski, J. W. Tashman, T. J. Hinton, S. Yerneni, J. M. Bliley, P. G. Campbell, A. W. Feinberg, *Science* **2019**, *365*, 482.
[187] C. B. Highley, C. B. Rodell, J. A. Burdick, *Adv Mater* **2015**, *27*, 5075.
[188] M. Albanna, K. W. Binder, S. V. Murphy, J. Kim, S. A. Qasem, W. Zhao, J. Tan, I. B. El-Amin, D. D. Dice, J. Marco, J. Green, T. Xu, A. Skardal, J. H. Holmes, J. D. Jackson, A. Atala, J. J. Yoo, *Sci Rep* **2019**, *9*, 1856.
[189] C. Di Bella, S. Duchi, C. D. O'Connell, R. Blanchard, C. Augustine, Z. Yue, F. Thompson, C. Richards, S. Beirne, C. Onofrillo, S. H. Bauquier, S. D. Ryan, P. Pivonka, G. G. Wallace, P. F. Choong, *J Tissue Eng Regen Med* **2018**, *12*, 611.
[190] X. Ma, X. Qu, W. Zhu, Y. S. Li, S. Yuan, H. Zhang, J. Liu, P. Wang, C. S. Lai, F. Zanella, G. S. Feng, F. Sheikh, S. Chien, S. Chen, *Proc Natl Acad Sci U S A* **2016**, *113*, 2206.
[191] W. Zhu, X. Qu, J. Zhu, X. Ma, S. Patel, J. Liu, P. Wang, C. S. Lai, M. Gou, Y. Xu, K. Zhang, S. Chen, *Biomaterials* **2017**, *124*, 106.

[192] B. Grigoryan, S. J. Paulsen, D. C. Corbett, D. W. Sazer, C. L. Fortin, A. J. Zaita, P. T. Greenfield, N. J. Calafat, J. P. Gounley, A. H. Ta, F. Johansson, A. Randles, J. E. Rosenkrantz, J. D. Louis-Rosenberg, P. A. Galie, K. R. Stevens, J. S. Miller, *Science* **2019**, *364,* 458.
[193] K. Jakab, C. Norotte, B. Damon, F. Marga, A. Neagu, C. L. Besch-Williford, A. Kachurin, K. H. Church, H. Park, V. Mironov, R. Markwald, G. Vunjak-Novakovic, G. Forgacs, *Tissue Eng Part A* **2008**, *14,* 413.
[194] K. Jakab, C. Norotte, F. Marga, K. Murphy, G. Vunjak-Novakovic, G. Forgacs, *Biofabrication* **2010**, *2,* 022001.
[195] M. Itoh, K. Nakayama, R. Noguchi, K. Kamohara, K. Furukawa, K. Uchihashi, S. Toda, J. Oyama, K. Node, S. Morita, *PLoS One* **2015**, *10,* e0145971.
[196] O. Jeon, Y. B. Lee, H. Jeong, S. J. Lee, D. Wells, E. Alsberg, *Materials Horizons* **2019**, *6,* 1625.
[197] W. Yang, H. Yu, G. Li, Y. Wang, L. Liu, *Small* **2017**, *13,* 1602769.
[198] N. D. Dinh, R. Luo, M. T. A. Christine, W. N. Lin, W. C. Shih, J. C. Goh, C. H. Chen, *Small* **2017**, *13,* 1700684.
[199] J. P. K. Armstrong, M. M. Stevens, *Trends Biotechnol* **2019**, *in press,* doi.org/10.1016/j.tibtech.2019.07.005.
[200] V. Marx, *Nat Methods* **2015**, *12,* 41.
[201] A. Ozcelik, J. Rufo, F. Guo, Y. Gu, P. Li, J. Lata, T. J. Huang, *Nat Methods* **2018**, *15,* 1021.
[202] J. P. K. Armstrong, S. A. Maynard, I. J. Pence, A. C. franklin, B. W. drinkwater, M. M. Stevens, *Lab Chip* **2019**, *19,* 562.
[203] A. Tait, P. Glynne-Jones, A. R. Hill, D. E. Smart, C. Blume, B. Hammarstrom, A. L. Fisher, M. C. Grossel, E. J. Swindle, M. Hill, D. E. Davies, *Sci Rep* **2019**, *9,* 9789.
[204] K. Chen, M. Wu, F. Guo, P. Li, C. Y. Chan, Z. Mao, S. Li, L. Ren, R. Zhang, T. J. Huang, *Lab Chip* **2016**, *16,* 2636.
[205] K. Olofsson, V. Carannante, M. Ohlin, T. Frisk, K. Kushiro, M. Takai, A. Lundqvist, B. Onfelt, M. Wiklund, *Lab Chip* **2018**, *18,* 2466.
[206] Y. Wu, Z. Ao, C. Bin, M. Muhsen, M. Bondesson, X. Lu, F. Guo, *Nanotechnology* **2018**, *29,* 504006.
[207] S. Li, P. Glynne-Jones, O. G. Andriotis, K. Y. Ching, U. S. Jonnalagadda, R. O. Oreffo, M. Hill, R. S. Tare, *Lab Chip* **2014**, *14,* 4475.
[208] P. Chen, S. Guven, O. B. Usta, M. L. Yarmush, U. Demirci, *Adv Healthc Mater* **2015**, *4,* 1937.
[209] K. Melde, E. Choi, Z. Wu, S. Palagi, T. Qiu, P. Fischer, *Adv Mater* **2018**, *30,* 1704507.
[210] K. Melde, A. G. Mark, T. Qiu, P. Fischer, *Nature* **2016**, *537,* 518.
[211] K. A. Garvin, D. C. Hocking, D. Dalecki, *Ultrasound Med Biol* **2010**, *36,* 1919.
[212] K. A. Garvin, D. Dalecki, D. C. Hocking, *Ultrasound Med Biol* **2011**, *37,* 1853.
[213] E. S. Comeau, D. C. Hocking, D. Dalecki, *J Cell Sci* **2017**, *130,* 232.
[214] C. Bouyer, P. Chen, S. Guven, T. T. Demirtas, T. J. F. Nieland, F. Padilla, U. Demirci, *Adv Mater* **2016**, *28,* 161.
[215] S. M. Naseer, A. Manbachi, M. Samandari, P. Walch, Y. Gao, Y. S. Zhang, F. Davoudi, W. Wang, K. Abrinia, J. M. Cooper, A. Khademhosseini, S. R. Shin, *Biofabrication* **2017**, *9,* 015020.
[216] V. Serpooshan, P. Chen, H. Wu, S. Lee, A. Sharma, D. A. Hu, S. Venkatraman, A. V. Ganesan, O. B. Usta, M. Yarmush, F. Yang, J. C. Wu, U. Demirci, S. M. Wu, *Biomaterials* **2017**, *131,* 47.
[217] J. P. K. Armstrong, J. L. Puetzer, A. Serio, A. G. Guex, M. Kapnisi, A. Breant, Y. Zong, V. Assal, S. C. Skaalure, O. King, T. Murty, C. Meinert, A. C. Franklin, P. G. Bassindale, M. K. Nichols, C. M. Terracciano, D. W. Hutmacher, B. W. Drinkwater, T. J. Klein, A. W. Perriman, M. M. Stevens, *Adv Mater* **2018**, *30,* 1802649.
[218] B. Kang, J. Shin, H. J. Park, C. Rhyou, D. Kang, S. J. Lee, Y. S. Yoon, S. W. Cho, H. Lee, *Nat Commun* **2018**, *9,* 5402.
[219] P. Brown, A. M. Khan, J. P. K. Armstrong, A. W. Perriman, C. P. Butts, J. Eastoe, *Adv Mater* **2012**, *24,* 6244.
[220] L. J. Santos, R. L. Reis, M. E. Gomes, *Trends Biotechnol* **2015**, *33,* 471.
[221] C. Li, J. P. Armstrong, I. J. Pence, W. Kit-Anan, J. L. Puetzer, S. Correia Carreira, A. C. Moore, M. M. Stevens, *Biomaterials* **2018**, *176,* 24.
[222] S. Correia Carreira, J. P. Armstrong, M. Okuda, A. M. Seddon, A. W. Perriman, W. Schwarzacher, *J Vis Exp* **2016**, *118,* 54785.
[223] A. Ito, Y. Takizawa, H. Honda, K. I. Hata, H. Kagami, M. Ueda, T. Kobayashi, *Tissue Eng Part A* **2004**, *10,* 833.
[224] A. Ito, E. Hibino, C. Kobayashi, H. Terasaki, H. Kagami, M. Ueda, T. Kobayashi, H. Honda, *Tissue Eng* **2005**, *11,* 489.
[225] Y. Yamamoto, A. Ito, M. Kato, Y. Kawabe, K. Shimizu, H. Fujita, E. Nagamori, M. Kamihira, *J Biosci Bioeng* **2009**, *108,* 538.

[226] Y. Yamamoto, A. Ito, H. Fujita, E. Nagamori, Y. Kawabe, M. Kamihira, *Tissue Eng Part A* **2011**, *17,* 107.
[227] A. Ito, K. Ino, M. Hayashida, T. Kobayashi, H. Matsunuma, H. Kagami, M. Ueda, H. Honda, *Tissue Eng Part A* **2005**, *11,* 1553.
[228] W. Zhang, G. Yang, X. Wang, L. Jiang, F. Jiang, G. Li, Z. Zhang, X. Jiang, *Adv Mater* **2017**, *29,* 1703795.
[229] K. Ino, A. Ito, H. Honda, *Biotechnol Bioeng* **2007**, *97,* 1309.
[230] H. Akiyama, A. Ito, Y. Kawabe, M. Kamihira, *Biomed Microdevices* **2009**, *11,* 713.
[231] V. Du, N. Luciani, S. Richard, G. Mary, C. Gay, F. Mazuel, M. Reffay, P. Menasche, O. Agbulut, C. Wilhelm, *Nat Commun* **2017**, *8,* 400.
[232] C. Adine, K. K. Ng, S. Rungarunlert, G. R. Souza, J. N. Ferreira, *Biomaterials* **2018**, *180,* 52.
[233] G. R. Souza, J. R. Molina, R. M. Raphael, M. G. Ozawa, D. J. Stark, C. S. Levin, L. F. Bronk, J. S. Ananta, J. Mandelin, M. M. Georgescu, J. A. Bankson, J. G. Gelovani, T. C. Killian, W. Arap, R. Pasqualini, *Nat Nanotechnol* **2010**, *5,* 291.
[234] M. Pottler, A. Fliedner, J. Bergmann, L. K. Bui, M. Muhlberger, C. Braun, M. Graw, C. Janko, O. Friedrich, C. Alexiou, S. Lyer, *Tissue Eng Part A* **2019**, *25,* 1470.
[235] A. C. Daquinag, G. R. Souza, M. G. Kolonin, *Tissue Eng Part C Methods* **2013**, *19,* 336.
[236] E. E. Lewis, H. Wheadon, N. Lewis, J. Yang, M. Mullin, A. Hursthouse, D. Stirling, M. J. Dalby, C. C. Berry, *ACS Nano* **2016**, *10,* 8346.
[237] H. Tseng, L. R. Balaoing, B. Grigoryan, R. M. Raphael, T. C. Killian, G. R. Souza, K. J. Grande-Allen, *Acta Biomater* **2014**, *10,* 173.
[238] H. Tseng, J. A. Gage, R. M. Raphael, R. H. Moore, T. C. Killian, K. J. Grande-Allen, G. R. Souza, *Tissue Eng Part C-Methods* **2013**, *19,* 665.
[239] S. Tasoglu, D. Kavaz, U. A. Gurkan, S. Guven, P. Chen, R. Zheng, U. Demirci, *Adv Mater* **2013**, *25,* 1137.
[240] S. Tasoglu, C. H. Yu, V. Liaudanskaya, S. Guven, C. Migliaresi, U. Demirci, *Adv Healthc Mater* **2015**, *4,* 1469.
[241] E. R. Ruskowitz, C. A. DeForest, *Nat Rev Mater* **2018**, *3,* 1.
[242] J. R. Moffitt, Y. R. Chemla, S. B. Smith, C. Bustamante, *Annu Rev Biochem* **2008**, *77,* 205.
[243] S. N. Olof, J. A. Grieve, D. B. Phillips, H. Rosenkranz, M. L. Yallop, M. J. Miles, A. J. Patil, S. Mann, D. M. Carberry, *Nano Lett* **2012**, *12,* 6018.
[244] J. P. K. Armstrong, S. N. Olof, M. D. Jakimowicz, A. P. Hollander, S. Mann, S. A. Davis, M. J. Miles, A. J. Patil, A. W. Perriman, *Chemical Science* **2015**, *6,* 6106.
[245] A. Linnenberger, C. Fiedler, J. J. Roberts, S. C. Skaalure, S. J. Bryant, M. C. Cole, R. R. McLeod, *Optical Trapping and Optical Micromanipulation X* **2013**, *8810*.
[246] G. R. Kirkham, E. Britchford, T. Upton, J. Ware, G. M. Gibson, Y. Devaud, M. Ehrbar, M. Padgett, S. Allen, L. D. Buttery, K. Shakesheff, *Sci Rep* **2015**, *5,* 8577.
[247] G. M. Akselrod, W. Timp, U. Mirsaidov, Q. Zhao, C. Li, R. Timp, K. Timp, P. Matsudaira, G. Timp, *Biophys J* **2006**, *91,* 3465.
[248] U. Mirsaidov, J. Scrimgeour, W. Timp, K. Beck, M. Mir, P. Matsudaira, G. Timp, *Lab Chip* **2008**, *8,* 2174.
[249] D. J. Odde, M. J. Renn, *Trends Biotechnol* **1999**, *17,* 385.
[250] D. J. Odde, M. J. Renn, *Biotechnol Bioeng* **2000**, *67,* 312.
[251] Y. Nahmias, R. E. Schwartz, C. M. Verfaillie, D. J. Odde, *Biotechnol Bioeng* **2005**, *92,* 129.
[252] Y. Nahmias, D. J. Odde, *Nat Protoc* **2006**, *1,* 2288.
[253] S. Yüz, S. Rasoulinejad, M. Mueller, A. E. Wegner, S. V. Wegner, *Advanced Biosystems* **2019**, *3,* 1800310.
[254] P. Q. Nguyen, N. D. Courchesne, A. Duraj-Thatte, P. Praveschotinunt, N. S. Joshi, *Adv Mater* **2019**, *30,* 1704847.
[255] J. J. Hay, A. Rodrigo-Navarro, M. Petaroudi, A. V. Bryksin, A. J. Garcia, T. H. Barker, M. J. Dalby, M. Salmeron-Sanchez, *Adv Mater* **2018**, *30,* 1804310.
[256] S. Sankaran, S. Zhao, C. Muth, J. Paez, A. Del Campo, *Adv Sci (Weinh)* **2018**, *5,* 1800383.
[257] M. Evander, J. Nilsson, *Lab Chip* **2012**, *12,* 4667.
[258] A. M. Blakely, K. L. Manning, A. Tripathi, J. R. Morgan, *Tissue Eng Part C Methods* **2015**, *21,* 737.
[259] H. P. Wang, Q. Shi, M. Nakajima, M. Takeuchi, T. Chen, P. Di, Q. Huang, T. Fukuda, *Int J Adv Robot Syst* **2014**, *11,* 121.
[260] A. Yusof, H. Keegan, C. D. Spillane, O. M. Sheils, C. M. Martin, J. J. O'Leary, R. Zengerle, P. Koltay, *Lab Chip* **2011**, *11,* 2447.
[261] K. Zhu, N. Chen, X. Liu, X. Mu, W. J. Zhang, C. S. Wang, Y. S. Zhang, *Macromol Biosci* **2018**, *18,* e1800127.

[262] N. Noor, A. Shapira, R. Edri, I. Gal, L. Wertheim, T. Dvir, *Adv Sci (Weinh)* **2019**, *6,* 1900344.
[263] M. A. Skylar-Scott, S. G. M. Uzel, L. L. Nam, J. H. Ahrens, R. L. Truby, S. Damaraju, J. A. Lewis, *Sci Adv* **2019**, *5,* eaaw2459.
[264] J. S. Miller, K. R. Stevens, M. T. Yang, B. M. Baker, D. H. Nguyen, D. M. Cohen, E. Toro, A. A. Chen, P. A. Galie, X. Yu, R. Chaturvedi, S. N. Bhatia, C. S. Chen, *Nat Mater* **2012**, *11,* 768.
[265] D. B. Kolesky, K. A. Homan, M. A. Skylar-Scott, J. A. Lewis, *Proc Natl Acad Sci U S A* **2016**, *113,* 3179.
[266] L. Ouyang, J. P. K. Armstrong, Q. Chen, Y. Lin, M. M. Stevens, *Adv Funct Mater* **2019**, *In press,* doi.org/10.1002/adfm.201908349.

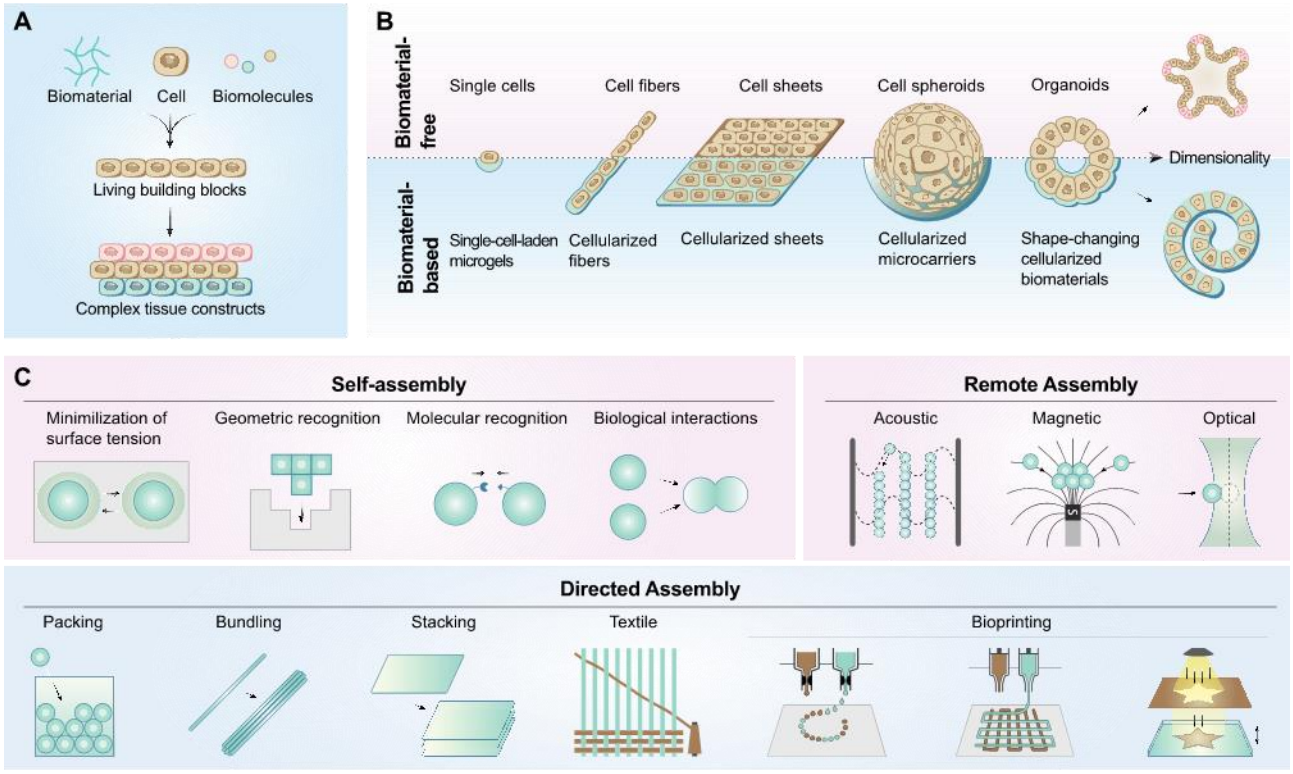

Figure 1. An overview of different bottom-up tissue engineering strategies. (A) Living building blocks are fabricated using cells, together with optional biomaterials and biomolecules, and then assembled into complex tissue constructs. (B) An illustration of the different multi-dimensional living building blocks, ranging from zero-dimensional single cell units to four-dimensional dynamic multicellular units. Biomaterial-free and biomaterial-based categories are indicated. (C) A schematic of representative techniques for living building block assembly, categorized into self-assembly, directed assembly, and remote assembly.

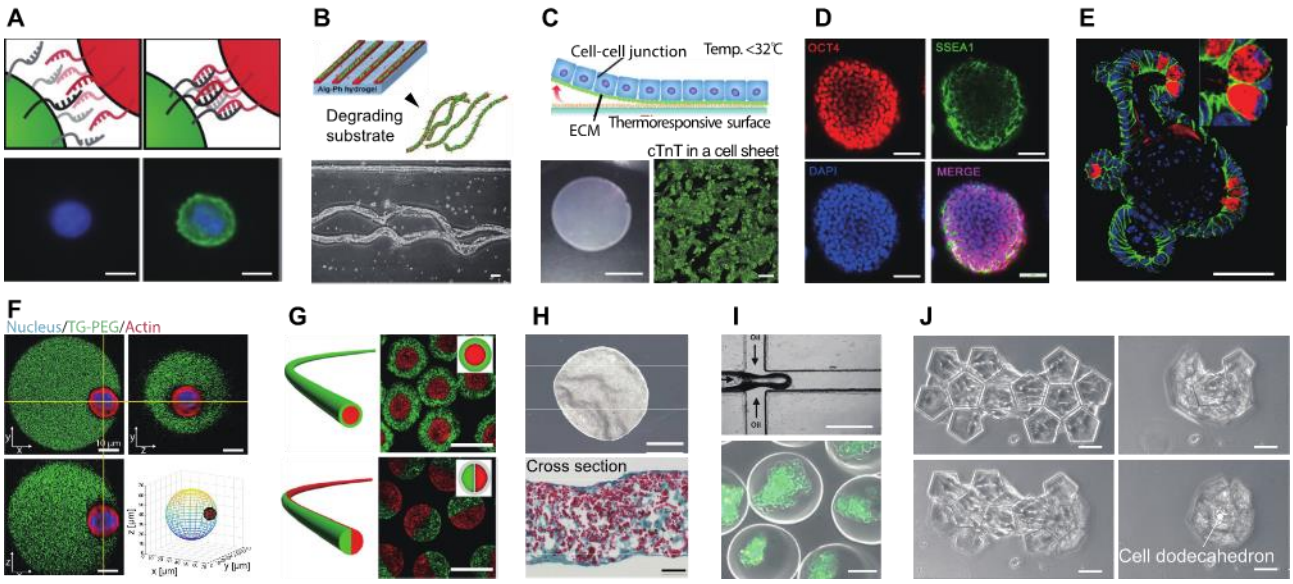

Figure 2. Representative examples of **living building blocks**. (A) Single cells functionalized with fluorescein-conjugated DNA (green, bottom-right) and a nonfluorescent complementary strand (bottom-left). Scale bars: 10 μm. Reproduced with permission. [20] Copyright 2009, National Academy of Sciences. (B) Cell fibers fabricated by releasing fibroblasts cultured on a patterned culture substrate. Reproduced with permission. [32] Copyright 2020, IOP Publishing. (C) Cardiac cell sheets harvested using thermally-triggered detachment. Scale bars: 1 mm (bottom-left), 100 μm (bottom-right). Reproduced with permission. [38] Copyright 2012, Elsevier. (D) A pluripotent embryoid body generated from a 3D cell culture system. Scale bars: 50 μm. Reproduced with permission. [49] Copyright 2016, IOP Publishing. (E) An intestinal organoid formed in a synthetic PEG-based matrix. Scale bar: 50 μm. Reproduced with permission. [56] Copyright 2016, Springer Nature. (F) Single cell-encapsulated microgels generated by selective crosslinking of cell-laden PEG microdroplets in a microfluidic device. Scale bars: 10 μm. Reproduced with permission. [65] Copyright 2017, Royal Society of Chemistry. (G) Core-shell and half-half cellularized alginate hydrogel fibers generated from capillary microfluidics. Scale bars: 200 μm. Reproduced with permission. [70] Copyright 2018, Springer Nature. (H) Cellular sheets made of collagen microparticles and fibroblasts. Scale bars: 2 mm (top), 100 μm (bottom). Reproduced with permission. [82] Copyright 2017, American Chemical Society. (I) Fibroblast-laden GelMA microgels generated using a microfluidic device. Scale bars: 500 μm (top), 100 μm (bottom). Reproduced with permission. [97] Copyright 2019, Royal Society of Chemistry. (J) Shape-changing cellularized units, with changes driven by cell traction. Scale bars: 50 μm. Reproduced with permission. [114] Copyright 2012, Kuribayashi-Shigetomi *et al*.

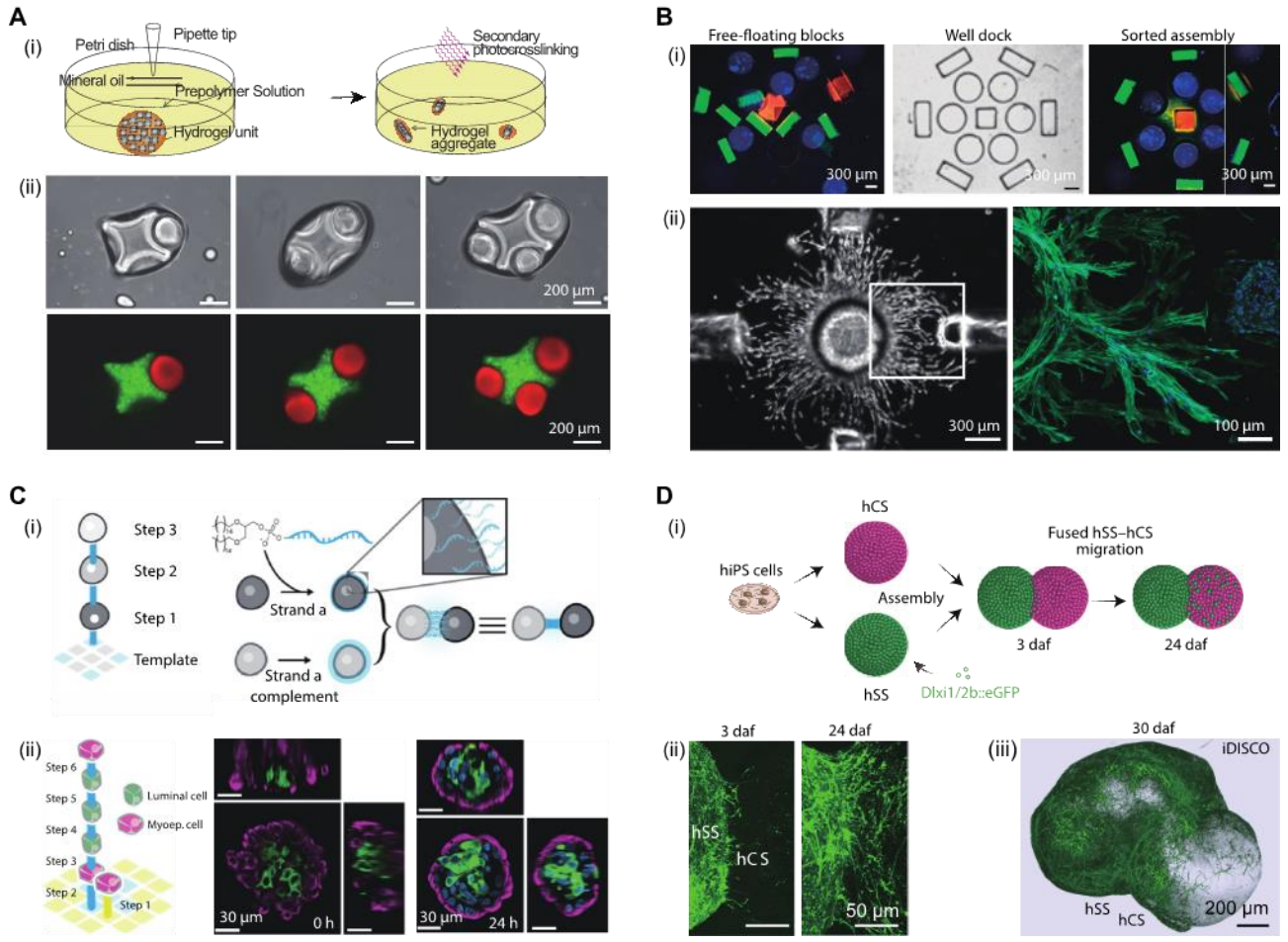

Figure 3. Representative approaches for the **self-assembly** of living building blocks. (A) (i) Schematic of the spontaneous assembly of cellular microgels, driven by the tendency to minimize surface tension in multiphase liquid–liquid systems. (ii) Examples of some multi-module structures formed using this method. Scale bars: 200 µm. Reproduced with permission. [106] Copyright 2008, National Academy of Sciences. (B) (i) An example of geometric recognition, in which defined cellular microenvironments are formed by the spontaneous assembly of shape-coded hydrogels into conjugate wells. (ii) This method was used to generate defined assemblies of human mesenchymal stem cells and endothelial cells, shown here after 14 days of co-culture. Scale bars: 300 µm. Reproduced with permission. [120] Copyright 2013, National Academy of Sciences. (C) (i) Schematic of a multistep DNA-programmed assembly process based on complementary cell-surface oligonucleotides. (ii) Schematic and images of assembled aggregates of human luminal and myoepithelial cells embedded in Matrigel. Scale bars: 30 µm. Reproduced with permission. [129] Copyright 2015, Springer Nature. (D) (i) Biological interactions mediating the fusion of human cortical spheroids (hCS) and human subpallium spheroids (hSS). (ii) Time-lapse microscopy of neuronal migration from hSS into hCS. (iii) This process was used to generate hybrid cerebral microtissues, shown here after 30 days in culture. Scale bars: 50 µm (ii), 200 µm (iii). Reproduced with permission. [137] Copyright 2017, Springer Nature.

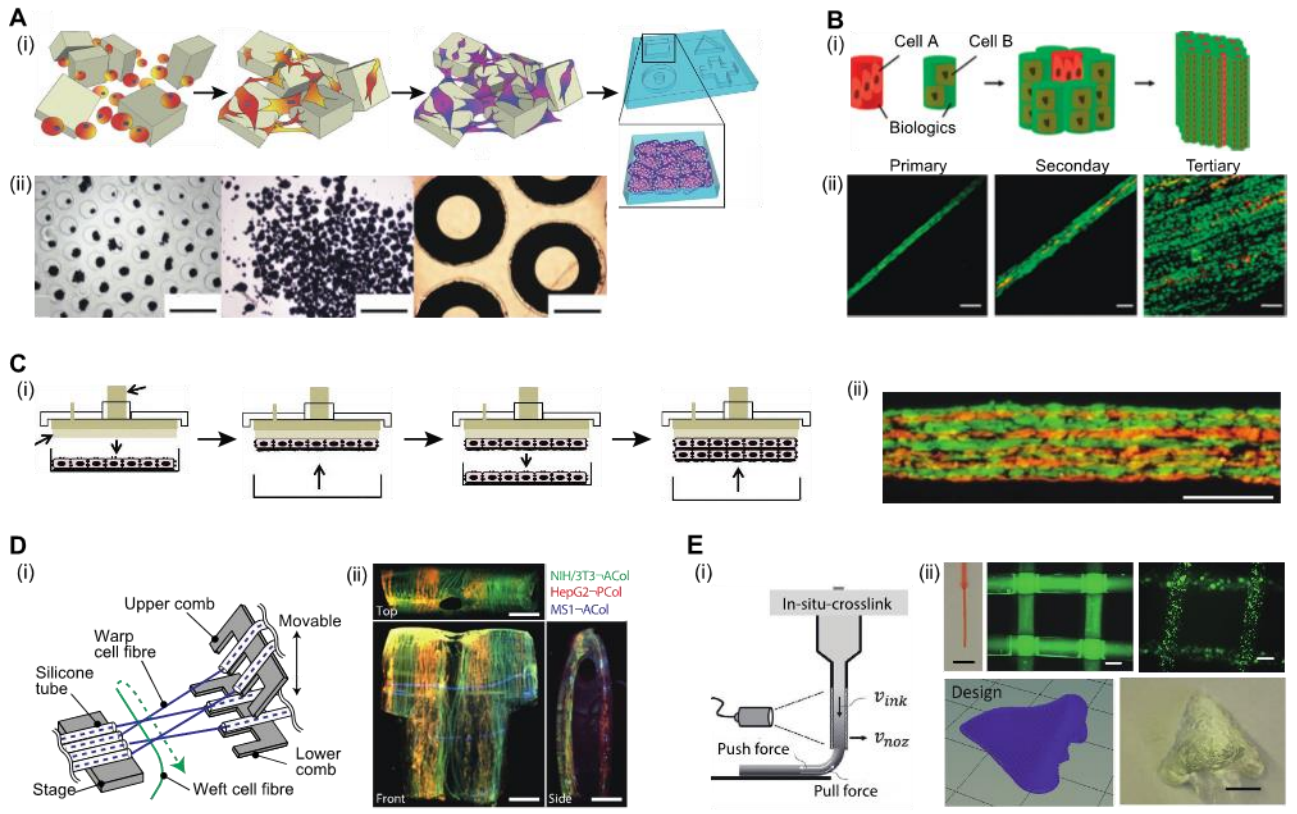

Figure 4. Representative approaches for the **directed assembly** of living building blocks. (A) (i) Schematic of cell-seeded microcarriers packed into customized molds. (ii) Packed spherical building blocks assembled into bigger ring-shaped constructs. Scale bars: 1 mm. Reproduced with permission. [89] Copyright 2014, John Wiley and Sons. (B) (i) Schematic of a hierarchical structure generated by bundling parallel cell-laden fibers. (ii) This technique was used to assemble anisotropic tissue constructs. Scale bars: 50 μm. Reproduced with permission. [146] Copyright 2013, Springer Nature. (C) (i) Schematic of cell sheet stacking using a plunger-like manipulator. (ii) This method was used to assemble multilayered tissue. Scale bar: 100 μm. Reproduced with permission. [149] Copyright 2012, Springer Nature. (D) (i) Schematic of a weaving fabrication method using cell-laden hydrogel fibers. (ii) The woven tissue was post-processed to create folded 3D macroscopic cellular structures. Scale bars: 1 mm. Reproduced with permission. [71] Copyright 2013, Springer Nature. (E) (i) Schematic of an *in-situ* crosslinking strategy for bioprinting non-viscous, photo-crosslinkable bioinks. (ii) This method was used to assemble cell-laden hydrogel fibers into 3D lattices and a nasal geometry. Scale bars: 5 mm (top-left, bottom-right), 500 μm (top-middle, top-right). Reproduced with permission. [77] Copyright 2017, John Wiley and Sons.

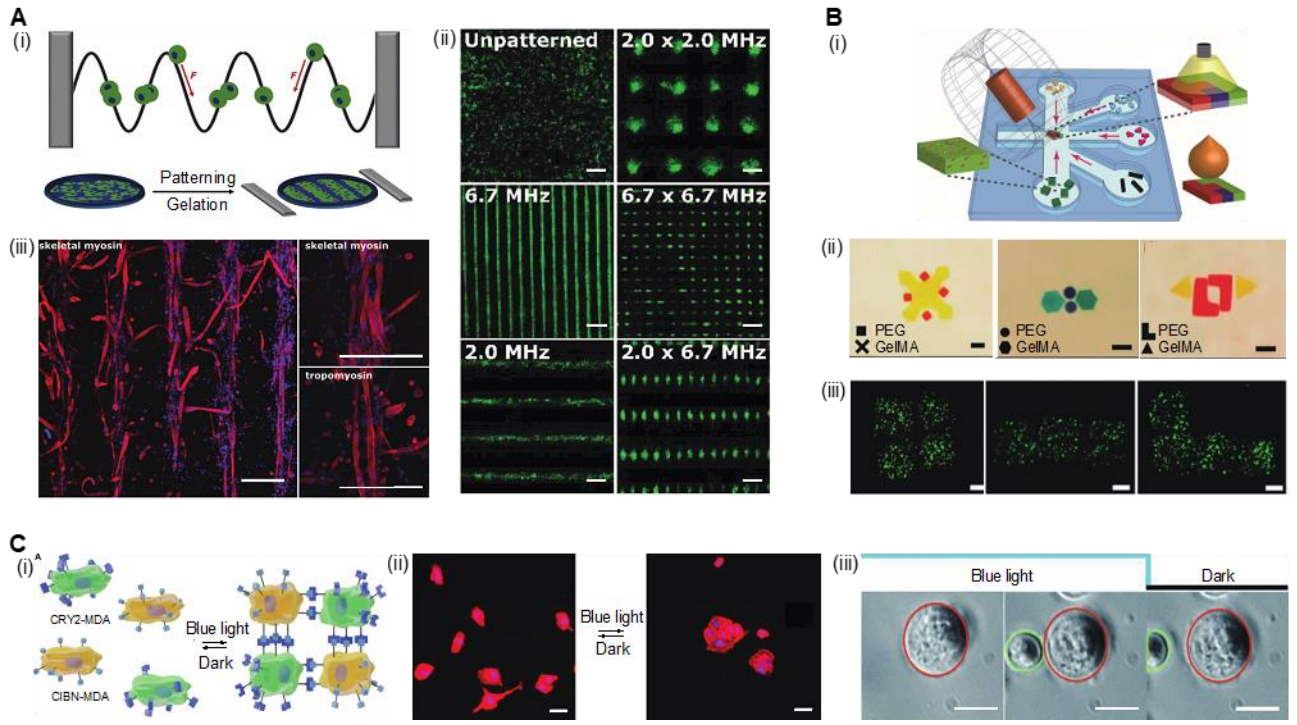

Figure 5. Representative approaches for the **remote assembly** of living building blocks. (A) (i) Schematic of acoustic cell pattering by ultrasound standing waves. (ii) Fluorescence microscopy of skeletal myoblasts (green) patterned under different acoustic fields in suspension. (iii) Immunostaining for α-myosin skeletal fast and tropomyosin (both red) in the patterned skeletal muscle tissue at day 7. Scale bars: 300 μm (i), 200 μm (ii). Reproduced with permission. [217] Copyright 2018, Armstrong *et al*. (B) (i) Schematic of the guided assembly of magnetoceptive hydrogels using a permanent NdFeB magnet on a liquid reservoir. (ii) This method was used to generate heterogeneous assemblies of PEGDMA and GelMA hydrogels. (iii) Fluorescent images of square, rod-shaped and L-shaped assemblies of fibroblasts-embedded GelMA. Scale bars: 1 mm (ii), 200 μm (iii). Reproduced with permission. [122] Copyright 2014, Springer Nature. (C) (i) An example of optical assembly in which blue light was used to trigger specific heterophilic interactions between cells expressing light switchable proteins CRY2 or CIBN on the surfaces. (ii) Cells cultured in the dark remain as single cells, but cells cultured under blue light form cell clusters due to CRY2-CIBN heterodimerization. (iii) Phase-contrast images from a time-lapse movie showing the binding of a CIBN-MDA cell (green cell) to CRY2-MDA cells (red circle) under blue light and its dissociation in the dark. Scale bars: 100 μm (ii), 25 μm (iii). Reproduced with permission. [253] Copyright 2019, John Wiley and Sons.

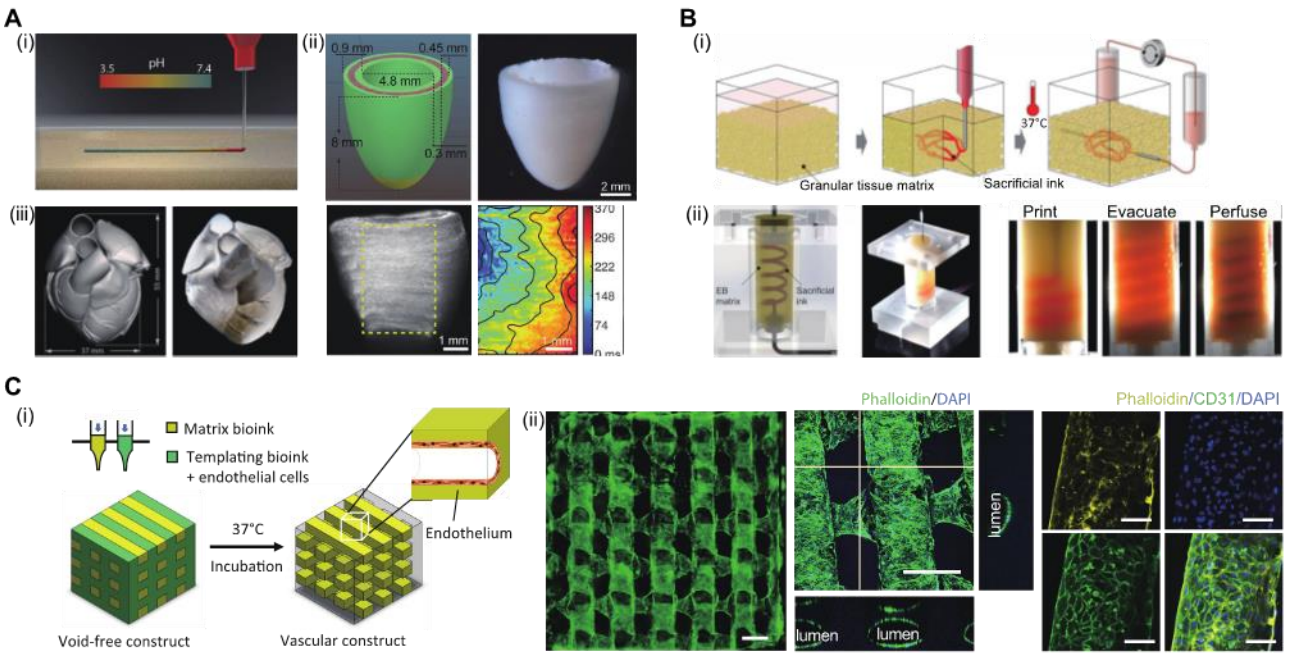

Figure 6. New opportunities in **bioprinting** for engineering complex tissues. (A) (i) Schematic of printing collagen into a granular supporting gel. This FRESH v2.0 assembly technique was used to fabricate: (ii) a functional ventricle and (iii) a human heart model. Scale bars: 2 mm (ii, top), 1 mm (ii, bottom). Reproduced with permission. [186] Copyright 2019, AAAS. (B) (i) Schematic of bioprinting sacrificial inks into a supporting tissue matrix comprising densely-packed organoids. (ii) This method was used to fabricate a tissue construct with spiral perfusable vessels. Reproduced with permission. [263] Copyright 2019, Skylar-Scott *et al*. (C) (i) Schematic of a void-free bioprinting approach for *in-situ* endothelialization. (ii) This process was used to produce constructs with an interconnected 3D network of endothelialized channels after one week of culture. Scale bars: 500 μm (ii, left, middle), 100 μm (ii, right). Reproduced with permission. [266] Copyright 2019, Ouyang *et al*.

Table 1. Classification of living building blocks and their representative fabrication methods

	Biomaterial-free	**Biomaterial-based**
Zero-dimensional	**Single cells:** - Chemical modification [20, 22-30, 123-125, 129, 253] - Biological modification [19]	**Single-cell-laden microgels:** - Microfluidics [59-65] - Droplet-based bioprinting [173-175]
One-dimensional	**Cell fibers:** - Patterned mold culture [33-35] - Patterned substrate culture [32]	**Cellularized biomaterial fibers:** - Molding [66] - Microfluidics [67-73] - Extrusion [74-77] - Cell electrospinning [79, 80]
Two-dimensional	**Cell sheets:** - Monolayer culture [36-43]	**Cellularized biomaterial sheets:** - Molding [83-85] - Microfluidics [86, 87] - Light projection [190-192]
Three-dimensional	**Cell spheroids:** - Microwell culture [15, 52, 141] - Suspension culture [44-47] - 3D encapsulation culture [49-51] - Hanging-drop culture [48] - Magnetic levitation [223-229, 233, 235, 237, 238] - Acoustic assembly [204, 206]	**Cellularized microcarriers:** - Molding [94, 105, 139] - Microfluidics [90-93, 96, 97, 101] - Two-phase emulsion [52] - Droplet-based bioprinting [168, 169, 171-173, 177] - Electro-spraying [102, 103] - Photolithography [106-109]
Four-dimensional	**Cell organoids:** - Suspension culture [55] - 3D encapsulation culture [54, 56-58]	**Shape-changing cellularized biomaterials:** - Extrusion-based bioprinting [113] - Bilayer construction [110-112, 114]

Table 2. Comparison of different assembly techniques

Assembly Techniques	Relevant examples of living building blocks	Advantages	Disadvantages
Self-assembly			
Minimization of surface tension	- Cellularized microgels [106, 115-118]	- Fast assembly - Readily scaled up	- Requires two phases - Poor spatial control
Geometric recognition	- Cellularized microgels [106, 116, 118, 120-122]	- Specific recognition - Simple operation	- Risk of recognition errors - Requires excess modules
Molecular recognition	- Single cells [20, 125, 129] - Cellularized microgels [126-128]	- Specific recognition - Can be programmable - Single cell resolution	- Requires functionalization - Challenging to scale up
Biological interactions	- Single cells [131] - Cell spheroids [132, 133] - Organoid [134-137]	- Biologically relevant interaction - High cell density	- Requires cell-cell contact - Unpredictable outcome due to biological variance
Directed assembly			
Packing	- Cell spheroids [132, 141, 142] - Cellularized microcarriers [88, 89, 138, 139, 143-145]	- Applicable to various living building blocks - Readily scaled up - Customized shape	- Challenging to generate interstitial porosity - Poor control over heterogenous assembly
Bundling	- Cell fibers [148] - Cellularized biomaterial fibers [73, 146, 147]	- Can be used to create assemblies with anisotropic properties - Readily scaled up	- Challenging to generate interstitial porosity - Poor structural complexity
Stacking	- Cell sheets [149, 150, 156] - Cellularized biomaterial sheets [85, 153-155, 157] - Cellularized microcarriers [107, 109, 152]	- Applicable to various living building blocks - Readily scaled up	- Imprecise positioning - Poor control over the vertical features
Textile-based assembly	- Cellularized biomaterial fibers [71, 164, 165]	- Can create complex interlacing networks - Can be used to create assemblies with anisotropic properties	- Requires specialized textile-based equipment - Challenging to create tight textile patterns
Bioprinting	- Single cells [173-175] - Cell fibers [140, 194, 196] - Cell spheroids [193, 195] - Cellularized gel fibers [77, 178-180, 182-189] - Cellularized gel sheets [190-192] - Cellularized microgels [168, 169, 171-173, 177]	- Free-form assembly - Applicable to various living building blocks - Can be used to create complex geometry and porosity in 3D - Rapid fabrication	- Requires “printable” formulations that enable deposition, crosslinking, structural stability and maintained cell viability - Requires specialized bioprinting equipment
Remote assembly			
Acoustic assembly	- Single cells [203-208, 211-218] - Cellularized microcarriers [121]	- High throughput and rapid assembly - Can generate complex geometric patterns - No labelling required	- Assembly can be impeded by opposing forces (*e.g.*, gravity, acoustic streaming, viscous forces)

Magnetic assembly	- Single cells [223-229, 235, 237, 238] - Cell sheets [237, 238] - Cellularized microcarriers [122, 239, 240]	- Can selectively assemble only magnetized living building blocks	- Limited to simple field attraction / repulsion - Requires cell labeling or paramagnetic media
Optical assembly	- Single cells [245-248, 250-253]	- Rapid and precise: can be used to assemble single cells	- Challenging to scale up - Potential for the laser to impact cell viability

Table 3. Comparison of different bioprinting techniques

Method of Bioprinting Living Building Blocks		Advantages	Disadvantages
Droplet-based bioprinting	- Using a cell suspension or cell-laden prepolymer solution to produce and assemble cellularized microcarriers [168, 169, 171-175, 177]	- High speed - High resolution - Low cost	- Challenging to assemble thick 3D structures - Narrow parameter space (*e.g.*, viscosity)
Extrusion-based bioprinting	- Using a cell suspension to produce cell fibers [140, 194, 196] - Using a cell-laden prepolymer to produce and assemble cellularized biomaterial fibers / microgels [77, 178-180, 182-189]	- Can assemble thick 3D structures - Can use different bioinks and crosslinking mechanisms - Different crosslinking approaches	- Low resolution - There can be poor adhesion between adjacent fibers or layers
Light-projection bioprinting	- Using a cell-laden hydrogel solution to produce and assemble cellularized biomaterial sheets [190-192]	- High speed - High resolution - Strong adhesion between adjacent layers	- Limited to photo-crosslinking - Challenging to assemble multiple cell types/hydrogels - Requires excess bioink
Spheroid bioprinting	- Directly assembling spheroids into tissue constructs [193, 195]	- Biologically relevant interaction - High cell density	- Requires temporary support (*e.g.*, biopaper, needle) - Low resolution